Mechanism Dictates Mechanics: A Molecular Substituent Effect in the Macroscopic Fracture of a Covalent Polymer Network

Shu Wang[†,‡], Haley K. Beech[†,‖], Brandon H. Bowser[†,‡], Tatiana B. Kouznetsova[†,‡], Bradley D. Olsen[*,†,‖], Michael Rubinstein[*,†,‡,§] and Stephen L. Craig[*,†,‡]

[†]NSF Center for the Chemistry of Molecularly Optimized Networks; [‡]Department of Chemistry, [§]Departments of Physics, Mechanical Engineering, and Biomedical Engineering, Duke University, Durham, North Carolina 27708, United States; [‖]Department of Chemical Engineering, Massachusetts Institute of Technology, Cambridge, Massachusetts 02139, United States;

ABSTRACT: The fracture of rubbery polymer networks involves a series of molecular events, beginning with conformational changes along the polymer backbone and culminating with a chain scission reaction. Here, we report covalent polymer gels in which the macroscopic fracture "reaction" is controlled by mechanophores embedded within mechanically active network strands. We synthesized poly(ethylene glycol) (PEG) gels through the end-linking of azide-terminated tetra-arm PEG (M_n = 5 kDa) with bis-alkyne linkers. Networks were formed under identical conditions, except that the bis-alkyne was varied to include either a *cis*-diaryl (**1**) or *cis*-dialkyl (**2**) linked cyclobutane mechanophore that acts as a mechanochemical "weak link" through a force-coupled cycloreversion. A control network featuring a bis-alkyne without cyclobutane (**3**) was also synthesized. The networks show the same linear elasticity (G' = 23~24 kPa, 0.1 – 100 Hz) and equilibrium mass swelling ratios (Q = 10~11 in tetrahydrofuran), but they exhibit tearing energies that span a factor of 8 (3.4 J·m^{-2}, 10.5 J·m^{-2}, and 27.1 J·m^{-2} for networks with **1**, **2**, and **3**, respectively). The difference in fracture energy is well aligned with the force-coupled scission kinetics of the mechanophores observed in single-molecule force spectroscopy experiments, implicating local resonance stabilization of a diradical transition state in the cycloreversion of **1** as a key determinant of the relative ease with which its network is torn. The connection between macroscopic fracture and small molecule reaction mechanism suggests opportunities for molecular understanding and optimization of polymer network behavior.

The fracture of rubbery covalent polymer networks limits the lifetime and utility of biomedical implants,[1] consumer products,[2] and soft devices for emerging applications.[3] Network fracture is most commonly perceived macroscopically, for example by how difficult it is to tear a contact lens relative to a piece of gelatin or an automobile tire. Concepts of very specific chemical reactivity are rarely invoked. The macroscopic event, however, comprises of a series of molecular events, including low energy conformational changes and higher energy bond stretching, that culminate in a covalent chemical reaction: the scission of network strands that bridge the growing crack plane. Thus, it should be possible to connect behaviors on two very different length scales: the local molecular structure (e.g., substituent effects) that dictate chemical reactivity, and the macroscopic tearing of bulk material. Here, we report covalent polymer gels in which the reactivity of a single functional group within a network strand dictates the fracture energy.

Our approach, described in Figure 1a, is to embed a mechanophore[4,5] into each elastically active strand of a polymer network, systematically varying the mechanochemical reactivity in the otherwise identical networks. We chose cyclobutane-based mechanophores[6–8] whose reactivity through scissile cycloreversion differs as a result of the substituent (aryl vs. methylene, dark vs. light blue in Figure 1b) on the cyclobutane ring. The mechanochemical reactivity of the diaryl cyclobutane was previously characterized by Weng and co-workers using single-molecule force spectroscopy (SMFS), and a force of 1.0 ± 0.1 nN is required to reduce the half-life for cycloreversion to ~40 ms.[9] We expected that converting the aryl substituents of **I** to

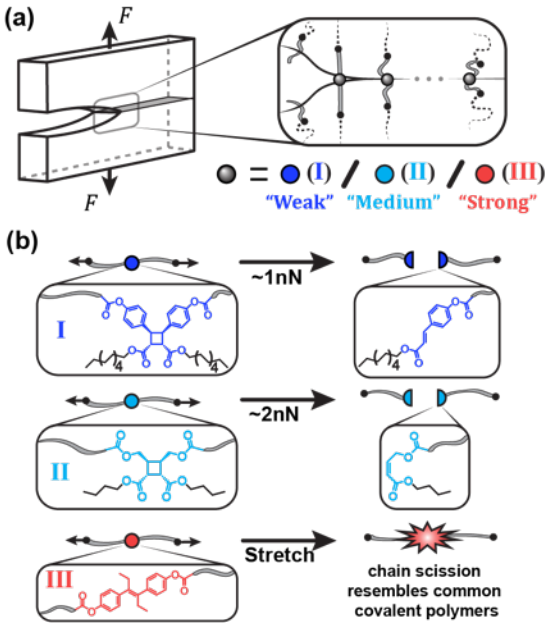

Figure 1. (a) Schematic illustration of embedding mechanochemically (**I**) "weak" and (**II**) "medium" mechanophores, and a mechanochemically (**III**) "strong" control structure into the otherwise identical networks. (b) Structures, force-coupled reactivities and the reaction mechanisms of **I** and **II**.

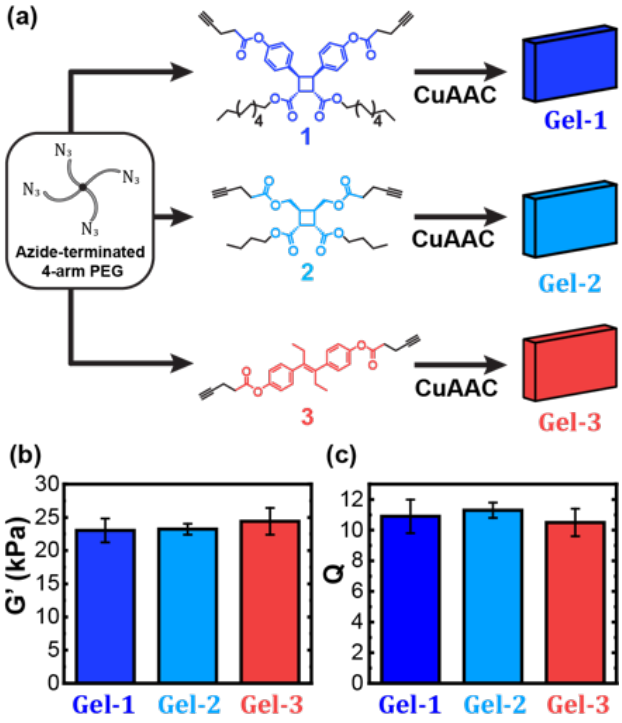

Figure 2. (a) Schematic illustration of gel preparation; all gels were prepared at the same condition. (b) Frequency sweeps of gels performed in the as-prepared state. (c) Equilibrium swelling ratios in THF.

methylenes in **II** would increase the force necessary for cycloreversion, and SMFS studies using methods reported previously[10,11] revealed that much larger forces (2.1 ± 0.1 nN) are required to achieve the same lability (See Supporting Information for polymer **PII**).

These mechanophores were incorporated into polymer networks as shown in **Figure 2**. Mechanophores **I** and **II** were incorporated into bis-alkyne linkers **1** and **2**, respectively (**Figure 2a**). A bis-alkyne linker (**3**) without cyclobutane was synthesized as a control. Linkers **1-3** were each then reacted via copper(I)-catalyzed azide-alkyne cycloaddition (CuAAC)[12,13] with azide-terminated tetra-arm PEG (M_n = 5 kDa), prepared as previously reported[14,15] to form the corresponding networks **Gel-1**, **Gel-2**, and **Gel-3**. Networks were formed under identical preparation conditions (25 mM PEG, alkyne : azide = 1 : 1, propylene carbonate as solvent). The preparation volume fraction $\phi_0 \approx 0.11$ was chosen to be just above the overlap volume fraction $\phi^* = 0.097$ and well below the entanglement volume fraction,[16,17] so that the load in every elastically active strand must be transmitted through a linker. Further details of the gel preparation can be found in Supporting Information.

We next verified that, aside from the content of the linker segment, **Gels 1-3** have effectively identical network structure. Shear moduli were measured with small amplitude oscillatory shear rheology in the as-prepared state. All three networks exhibit frequency-independent storage moduli G' across frequencies of 0.1-100 s^{-1}, and the average moduli of the networks are indistinguishable within experimental uncertainty across five different characterizations: 23.0 ± 1.8 kPa, 23.2 ± 0.8 kPa, and 24.4 ± 2.0 kPa, respectively (**Figure 2b**). The similar moduli indicate that the CuAAC polymerization is, as expected, similarly efficient across the networks, resulting in an indistinguishable number and distribution of elastically active strands. Further confirmation of structural homology comes from removing the propylene carbonate and immersing the formed networks in excess tetrahydrofuran; as with the elastic moduli, the equilibrium mass swelling ratios Q, defined as the mass ratio between the fully swollen and dry states, are statistically equivalent across four independent measurements: 10.9 ± 1.1, 11.3 ± 0.5, and 10.5 ± 0.9, respectively (**Figure 2c**).

We then characterized the impact of the embedded mechanophores on the strength of the network. A first indication of significant effect came from simply handling the materials; we were struck by the obvious differences in their tactile behavior. In particular, the texture of **Gel-1** is more fragile to the touch than **Gel-2** – to the point that it feels "crumbly" during sample transfer. Care is needed when introducing a notch to **Gel-1** with a razor blade for tear testing, as uncontrolled cuts result in the entire piece falling apart. In contrast, **Gel-2** is much easier to handle, but it still showed noticeably less resistance than **Gel-3** when cut with a punch or a razor blade. The gels have negligible differences in chemical composition and low strain, linear mechanical properties, and this qualitative observation suggested that there must be differences in mechanical properties that are associated with the behavior of the linkers at higher strains.

The stress-strain curves of unnotched and notched samples under uniaxial tension are shown in **Figure 3a,b**. As with the oscillatory rheology, the stress-strain behavior of the unnotched samples is identical up to the point of fracture, but the critical strain required for fracture (peak stress in the stress-strain curve) goes in the order **Gel-1** < **Gel-2** < **Gel-3**. The difference in strength is better quantified through the tearing energies, Γ, obtained from the strain necessary for the propagation of a crack introduced into notched samples.[18] Unlike the moduli, the tearing energies are significantly different across the gels: 3.4 ± 1.5 $J \cdot m^{-2}$, 10.6 ± 1.7 $J \cdot m^{-2}$, and 27.1 ± 1.6 $J \cdot m^{-2}$ for **Gel-1**, **Gel-2**, and **Gel-3**, respectively (**Figure 3c**).

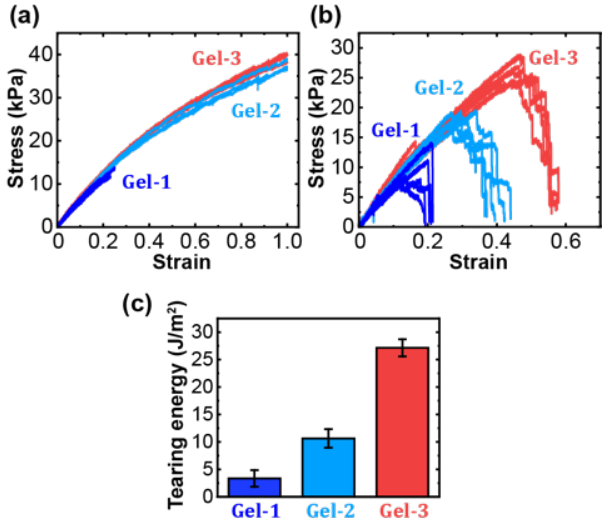

Figure 3. Stress-strain curves for (a) unnotched and (b) notched samples of **Gel 1-3**. (c) Tearing energies of **Gel 1-3**. All measurements were performed at the as-prepared state.

The difference in tearing energies is attributed to the only significant difference in the gels – the single mechanophore present in each linker. In strands made from **1** and **2**, the mechanical "weak bond"[19,20] is the cyclobutane mechanophore, whereas strands incorporating **3** are likely to undergo α-cleavage at the

C-C bond next to the 1,4-disubstituted 1,2,3-triazole ring.[21] The observed correlations highlight an important distinction. Molecular interpretations of polymer fracture energies, for example, those based on Lake-Thomas theory,[22] default to the thermodynamics of the bond scission reaction (e.g. total bond dissociation energy) as the relevant molecular thermodynamic quantity.[23,24] The systems employed here reveal limitations of this assumption, as the total BDEs (enthalpy of the cycloreversion reaction) for cyclobutane scission in **1** is exothermic,[9] and so fracture would require no energy. Instead, the relevant molecular parameters are associated with the kinetics of reactivity, as captured in SMFS measurements of force-coupled bond lifetimes for **1** and **2**. As noted above, the forces required for lifetimes of tens of ms are roughly 1 nN and 2 nN for **1** and **2**, respectively, whereas extrapolating prior calculations by Smalø and Uggerud gives a corresponding value of ~3 nN for triazole α-cleavage in **3**.[21] The actual loading rates at the propagating crack tips are unknown, preventing a more precise comparison, but the correlation with tearing energies is qualitatively consistent with recent adjustments to the Lake-Thomas theory.[25]

The results therefore suggest a direct connection between very tangible, macroscopic physical observables and quantum mechanical concepts of transient molecular electronic structure that cannot be observed directly. **Gel-1** and **Gel-2** are structurally identical, with the notable exception of the difference in aryl vs. methylene substituents at a single moiety in the linker connecting tetra-PEG macromers. The total aryl group content of **Gel-1** is 0.55 wt. % and immersed within a majority mobile solvent phase, and yet, as noted above, the two gels are easily distinguished by their feel to human touch. The difference in network properties that is actually being felt by hand, in essence, is the connection between tearing energy and the stabilization of a diradical cycloreversion transition state[9,26,27] by the aryl substituents, in large part through quantum mechanical effects manifested as resonance stabilization.[28]

Additional implications of these results include the opportunity to expand the use of mechanophores as quantitative probes of the molecular processes that underly polymer network fracture. Mechanochromic and mechanoluminescent mechanophores are providing molecular insights by enabling visualization of the damage zone,[29,30] and scissile mechanophores with known force-coupled reactivity complement those tools by connecting the structural observations to quantitative relationships between macroscopic and molecular mechanical responses. That opportunity motivates further characterizations of the force dependency of mechanochemical reactions[8,31–36] that are suited to this purpose, noting that historical connections between strand scission and bond dissociation energies are prone to error and become less valid as strands break through reaction mechanisms other than homolytic scission. This approach further motivates a better understanding of the relevant loading rate and associated reaction dynamics at the propagating crack tip. Such efforts might ultimately lead to quantitative, first-principles prediction of macroscopic fracture behavior as a function of network molecular structure.

ASSOCIATED CONTENT

Supporting Information. Synthetic procedures, gel preparation and characterizations, SMFS details. This material is available free of charge via the Internet at http://pubs.acs.org.

AUTHOR INFORMATION

Corresponding Author

*Bradley D. Olsen, bdolsen@mit.edu
*Michael Rubinstein, mr351@duke.edu
*Stephen L. Craig, stephen.craig@duke.edu

Funding Sources

This work was funded by the Center for the Chemistry of Molecularly Optimized Networks (MONET), a National Science Foundation (NSF) Center for Chemical Innovation (CHE-1832256) and Duke University.

Notes

The authors declare no competing financial interest.

ACKNOWLEDGMENT

This work was funded by the Center for the Chemistry of Molecularly Optimized Networks (MONET), a National Science Foundation (NSF) Center for Chemical Innovation (CHE-1832256) and Duke University.

REFERENCES

(1) De Coninck, T.; Huysse, W.; Willemot, L.; Verdonk, R.; Verstraete, K.; Verdonk, P. Two-Year Follow-up Study on Clinical and Radiological Outcomes of Polyurethane Meniscal Scaffolds. *Am. J. Sport. Med.* **2013**, *41*, 64–72.
(2) Mars, W. V.; Fatemi, A. A Literature Survey on Fatigue Analysis Approaches for Rubber. *Int. J. Fatigue* **2002**, *24* (9), 949–961.
(3) Root, S. E.; Savagatrup, S.; Printz, A. D.; Rodriquez, D.; Lipomi, D. J. Mechanical Properties of Organic Semiconductors for Stretchable, Highly Flexible, and Mechanically Robust Electronics. *Chem. Rev.* **2017**, *117* (9), 6467–6499.
(4) Izak-Nau, E.; Campagna, D.; Baumann, C.; Göstl, R. Polymer Mechanochemistry-Enabled Pericyclic Reactions. *Polym. Chem.* **2020**, *11*, 2274–2299.
(5) Ghanem, M. A.; Basu, A.; Behrou, R.; Boechler, N.; Boydston, A. J.; Craig, S. L.; Lin, Y.; Lynde, B. E.; Nelson, A.; Shen, H.; Storti, D. W. The Role of Polymer Mechanochemistry in Responsive Materials and Additive Manufacturing. *Nat. Rev. Mater.* **2020**, 1–15.
(6) Pill, M. F.; Holz, K.; Preusske, N.; Berger, F.; Clausen-Schaumann, H.; Luning, U.; Beyer, M. K. Mechanochemical Cycloreversion of Cyclobutane Observed at the Single Molecule Level. *Chem. Eur. J.* **2016**, *22* (34), 12034–12039.
(7) Wang, J.; Kouznetsova, T. B.; Boulatov, R.; Craig, S. L. Mechanical Gating of a Mechanochemical Reaction Cascade. *Nat. Commun.* **2016**, *7*, 13433.
(8) Tian, Y.; Cao, X.; Li, X.; Zhang, H.; Sun, C. L.; Xu, Y.; Weng, W.; Zhang, W.; Boulatov, R. A Polymer with Mechanochemically Active Hidden Length. *J. Am. Chem. Soc.* **2020**, *142* (43), 18687–18697.
(9) Zhang, H.; Li, X.; Lin, Y.; Gao, F.; Tang, Z.; Su, P.; Zhang, W.; Xu, Y.; Weng, W.; Boulatov, R. Multi-Modal Mechanophores Based on Cinnamate Dimers. *Nat. Commun.* **2017**, *8* (1), 1147.
(10) Bowser, B. H.; Craig, S. L. Empowering Mechanochemistry with Multi-Mechanophore Polymer Architectures. *Polym. Chem.* **2018**, *9* (26), 3583–3593.
(11) Zhang, Y.; Wang, Z.; Kouznetsova, T. B.; Sha, Y.; Xu, E.; Shannahan, L.; Fermen-Coker, M.; Lin, Y.; Tang, C.; Craig, S. L. Distal Conformational Locks on Ferrocene Mechanophores Guide Reaction Pathways for Increased Mechanochemical Reactivity. *Nat. Chem.* **2021**, *13*, 56–62.
(12) Rostovtsev, V. V.; Green, L. G.; Fokin, V. V.; Sharpless, K. B. A Stepwise Huisgen Cycloaddition Process: Copper(I)-Catalyzed Regioselective "Ligation" of Azides and Terminal Alkynes. *Angew. Chem., Int. Ed.* **2002**, *41* (14), 2596–2599.
(13) Malkoch, M.; Vestberg, R.; Gupta, N.; Mespouille, L.; Dubois, P.; Mason, A. F.; Hedrick, J. L.; Liao, Q.; Frank, C. W.; Kingsbury, K.; Hawker, C. J. Synthesis of Well-Defined Hydrogel Networks Using Click Chemistry. *Chem. Commun.* **2006**, 2774–2776.

(14) Zhong, M.; Wang, R.; Kawamoto, K.; Olsen, B. D.; Johnson, J. A. Quantifying the Impact of Molecular Defects on Polymer Network Elasticity. *Science* **2016**, *353* (6305), 1264–1268.
(15) Arora, A.; Lin, T.-S.; Beech, H. K.; Mochigase, H.; Wang, R.; Olsen, B. D. Fracture of Polymer Networks Containing Topological Defects. *Macromolecules* **2020**, *53*, 7346–7355.
(16) Akagi, Y.; Gong, J. P.; Chung, U.; Sakai, T. Transition between Phantom and Affine Network Model Observed in Polymer Gels with Controlled Network Structure. *Macromolecules* **2013**, *46* (3), 1035–1040.
(17) Rubinstein, M.; Colby, R. H. *Polymer Physics*; Oxford University Press: Oxford, U.K., 2003.
(18) Rivlin, R. S.; Thomas, A. G. Rupture of Rubber. I. Characteristic Energy for Tearing. *J. Polym. Sci.* **1953**, *10* (3), 291–318.
(19) Lee, B.; Niu, Z.; Wang, J.; Slebodnick, C.; Craig, S. L. Relative Mechanical Strengths of Weak Bonds in Sonochemical Polymer Mechanochemistry. *J. Am. Chem. Soc.* **2015**, *137* (33), 10826–10832.
(20) Berkowski, K. L.; Potisek, S. L.; Hickenboth, C. R.; Moore, J. S. Ultrasound-Induced Site-Specific Cleavage of Azo-Functionalized Poly(Ethylene Glycol). *Macromolecules* **2005**, *38*, 8975–8978.
(21) Smalø, H. S.; Uggerud, E. Ring Opening vs. Direct Bond Scission of the Chain in Polymeric Triazoles under the Influence of an External Force. *Chem. Commun.* **2012**, *48* (84), 10443–10445.
(22) Lake, G. J.; Thomas, A. G. The Strength of Highly Elastic Materials. *Proc. R. Soc. London, Ser. A Math. Phys. Sci.* **1967**, *300* (1460), 108–119.
(23) Akagi, Y.; Sakurai, H.; Gong, J. P.; Chung, U. I.; Sakai, T. Fracture Energy of Polymer Gels with Controlled Network Structures. *J. Chem. Phys.* **2013**, *139* (14), 144905.
(24) Mao, Y.; Talamini, B.; Anand, L. Rupture of Polymers by Chain Scission. *Extrem. Mech. Lett.* **2017**, *13*, 17–24.
(25) Wang, S.; Panyukov, S.; Rubinstein, M.; Craig, S. L. Quantitative Adjustment to the Molecular Energy Parameter in the Lake–Thomas Theory of Polymer Fracture Energy. *Macromolecules* **2019**, *52*, 2772–2777.
(26) Kean, Z. S.; Niu, Z.; Hewage, G. B.; Rheingold, A. L.; Craig, S. L. Stress-Responsive Polymers Containing Cyclobutane Core Mechanophores: Reactivity and Mechanistic Insights. *J. Am. Chem. Soc.* **2013**, *135* (36), 13598–13604.
(27) Chen, Z.; Mercer, J. A. M.; Zhu, X.; Romaniuk, J. A. H.; Pfattner, R.; Cegelski, L.; Martinez, T. J.; Burns, N. Z.; Xia, Y. Mechanochemical Unzipping of Insulating Polyladderene to Semiconducting Polyacetylene. *Science* **2017**, *357*, 475–479.
(28) Pauling, L. The Theory of Resonance in Chemistry. *Proc. R. Soc. London, Ser. A Math. Phys. Sci.* **1977**, *356*, 433–441.
(29) Ducrot, E.; Chen, Y.; Bulters, M.; Sijbesma, R. P.; Creton, C. Toughening Elastomers with Sacrificial Bonds and Watching Them Break. *Science* **2014**, *344* (6180), 186–189.
(30) Slootman, J.; Waltz, V.; Yeh, C. J.; Baumann, C.; Göstl, R.; Comtet, J.; Creton, C. Quantifying Rate- and Temperature-Dependent Molecular Damage in Elastomer Fracture. *Phys. Rev. X* **2020**, *10* (4), 041045.
(31) Akbulatov, S.; Tian, Y.; Huang, Z.; Kucharski, T. J.; Yang, Q.-Z.; Boulatov, R. Experimentally Realized Mechanochemistry Distinct from Force-Accelerated Scission of Loaded Bonds. *Science* **2017**, *357*, 299–303.
(32) Pill, M. F.; East, A. L. L.; Marx, D.; Beyer, M. K.; Clausen-Schaumann, H. Mechanical Activation Drastically Accelerates Amide Bond Hydrolysis, Matching Enzyme Activity. *Angew. Chem., Int. Ed.* **2019**, *58* (29), 9787–9790.
(33) Beedle, A. E. M.; Mora, M.; Davis, C. T.; Snijders, A. P.; Stirnemann, G.; Garcia-Manyes, S. Forcing the Reversibility of a Mechanochemical Reaction. *Nat. Commun.* **2018**, *9*, 3155.
(34) Huang, W.; Wu, X.; Gao, X.; Yu, Y.; Lei, H.; Zhu, Z.; Shi, Y.; Chen, Y.; Qin, M.; Wang, W.; Cao, Y. Maleimide–Thiol Adducts Stabilized through Stretching. *Nat. Chem.* **2019**, *11*, 310–319.
(35) Chen, Z.; Zhu, X.; Yang, J.; Mercer, J. A. M.; Burns, N. Z.; Martinez, T. J.; Xia, Y. The Cascade Unzipping of Ladderane Reveals Dynamic Effects in Mechanochemistry. *Nat. Chem.* **2020**, *12*, 302–309.
(36) Wollenhaupt, M.; Schran, C.; Krupička, M.; Marx, D. Force-Induced Catastrophes on Energy Landscapes: Mechanochemical Manipulation of Downhill and Uphill Bifurcations Explains the Ring-Opening Selectivity of Cyclopropanes. *ChemPhysChem* **2018**, *19* (7), 837–847.

Supporting information for

Mechanism Dictates Mechanics: A Molecular Substituent Effect in the Macroscopic Fracture of a Covalent Polymer Network

Shu Wang[†,‡], Haley K. Beech[†,‖], Brandon H. Bowser[†,‡], Tatiana B. Kouznetsova[†,‡], Bradley D. Olsen[*,†,‖], Michael Rubinstein[*,†,‡,§] and Stephen L. Craig[*,†,‡]

[†]NSF Center for the Chemistry of Molecularly Optimized Networks; [‡]Department of Chemistry, [§]Departments of Physics, Mechanical Engineering, and Biomedical Engineering, Duke University, Durham, North Carolina 27708, United States; [‖]Department of Chemical Engineering, Massachusetts Institute of Technology, Cambridge, Massachusetts 02139, United States

*Bradley D. Olsen, bdolsen@mit.edu
*Michael Rubinstein, mr351@duke.edu
*Stephen L. Craig, stephen.craig@duke.edu

Table of content

I. General procedures

1. Materials

Lab general solvents (dichloromethane, acetonitrile, hexane, ethyl acetate, acetone, tetrahydrofuran, dimethyl Sulfoxide) were purchased from VWR or Sigma Aldrich. 4-bromo-cinnamic acid, 1-Undecanol, 4- (dimethylamino)pyridine (DMAP), N,N'-Diisopropylcarbodiimide (DIC), Bis(pinacolato)diboron ($(Bpin)_2$), [1,1′-Bis(diphenylphosphino)ferrocene]dichloropalladium(II) complex with dichloromethane ($Pd(dppf)Cl_2$·DCM), potassium acetate (KOAc), acetic acid, 30% hydrogen peroxide, sodium metabisulfite, Maleic anhydride, cis-buten-1,4-diol, p-toluenesulfonic acid (pTSA), benzophenone, 1-butanol, 3-buten-1-ol, Grubbs II catalyst, palladium on carbon, 4-pentenoic anhydride, 9-oxabicyclo[6.1.0]non-4-ene, diethylstilbestrol were purchased from Sigma Aldrich or Alfa Aesar and used without further purification. 4-Pentynoic acid was purchased from Ambeed, Inc..

2. Characterizations

NMR and HRMS. ^1H NMR and ^{13}C NMR spectra were collected on a 400 MHz Bruker Avance or a 500 MHz Bruker spectrometer. ^1H shifts are reported as chemical shift, multiplicity, coupling constant if applicable, and relative integral. Multiplicities are reported as: singlet (s), doublet (d), doublet of doublets (dd), doublet of triplets (dt), doublet of doublet of doublets (ddd), doublet of doublet of triplets (ddt), triplet (t), triplet of doublets (td), quartet (q), multiplet (m), or broad (br). High-resolution mass spectra were collected on an Agilent LCMS-TOF-DART at Duke University's Mass Spectrometry Facility or an JEOL AccuTOF-DART at Massachusetts Institute of Technology's Mass Spectrometry Facility.

SMFS. The AFM pulling experiments were conducted in toluene at an ambient temperature (~23˚C) in the same manner as described previously[1–5] using a homemade AFM, which was constructed using a Bruker (previously Digital Instruments) Multimode AFM head mounted on top of a piezoelectric positioner (Physik Instrumente, GmbH), similar to the one described in detail previously.[6] Sharp Microlever silicon probes (MSNL) were purchased from Bruker (Camarillo, CA) and the force curves used for analysis were obtained with rectangular-shaped cantilevers (205 μm x 15 μm, nominal tip radius ~2 nm, nominal spring constant k ~ 0.02 N/m, frequency ~ 15 kHz). Multiple probes of the same type were used throughout the course of the experiments. The spring constant of each cantilever was calibrated in air, using the thermal noise method, based on the energy equipartition theorem as described previously.[7] Cantilever tips were prepared by soaking in piranha solution for ~15 min at room temperature. Silicon surfaces were prepared by soaking ~30 min in hot piranha solution, followed by washing with DI-water and drying under a stream of nitrogen.

The surface and cantilever were then placed in a UVO cleaner (ozone produced through UV light) for 15 min. After ozonolysis, the cantilever was mounted, and ~20 μL of a ~0.1-0.05 mg mL^{-1} polymer solution was added to the silicon surface and allowed to dry. Measurements were carried out in a fluid cell with scanning set for a series of constant velocity approaching/retracting cycles. To collect 'Force clamp' data cantilever deflection was monitored during each retraction cycle. If it reached threshold value corresponding to 200pN the system was switched to the force-control mode with the selected set point force value, which it attempted to keep for a set period of time (10-20sec), after which force-control mode was switched off and constant velocity retraction resumed to finish the 'pull'. During acquisition data were filtered at 500Hz. Force curves were collected in dSPACE (dSPACE Inc., Wixom, MI) and Matlab (The MathWorks, Inc., Natick, MA) and analyzed later using Matlab.

GPC. Gel permeation chromatography (GPC) was performed on two Agilent PLgel mixed-C columns (105 Å, 7.5x300 mm, 5 μm, part number PL1110-6500) using THF (stabilized with 100 ppm BHT) as the eluent. Molecular weights were calculated using a Wyatt Dawn EOS multi-angle light scattering (MALS) detector and Wyatt Optilab DSP Interferometric Refractometer (RI). The refractive index increment (dn/dc) values were determined by online calculation based on injections of known concentration and mass.

II. Synthesis

1. Synthesis of bis-alkyne linker 1

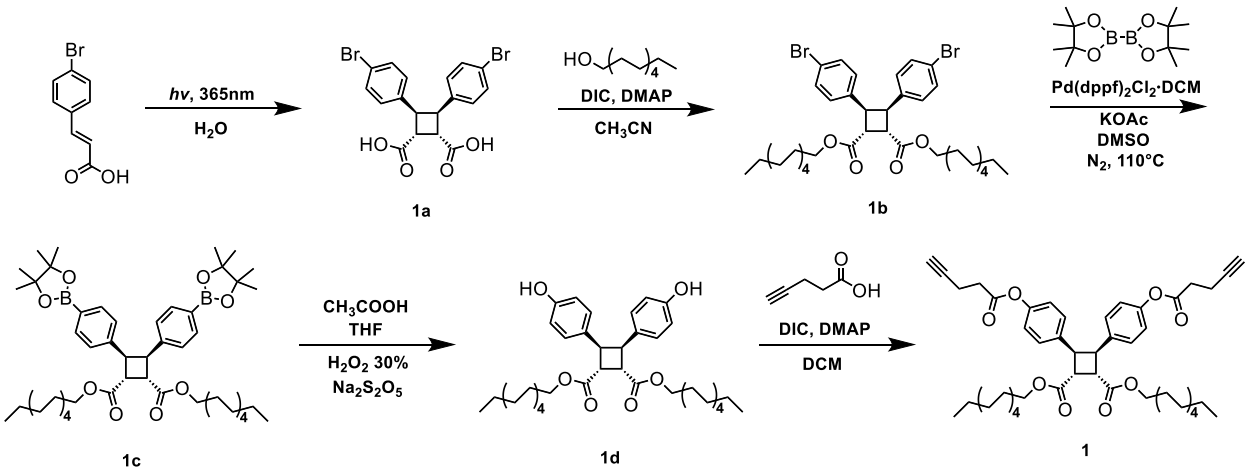

Scheme S1. Synthetic route of linker **1**.

Synthesis of 1a.[8] To a 2 L conical flask, around 1 L acetone was added and heated to boiling point. About 15 g of trans-4-bromo-cinnamic acid was added portion-wise to the boiling acetone. The mixture was stirred and heated until the solid was completely dissolved (more acetone was if the solid did not completely dissolve). The solution was cooled down at room temperature overnight to yield needle like β-trans-4-bromo-cinnamic acid crystal (metastable). The crystal was left at the bottom of the flask, while the acetone was poured into another conical flask for the future preparation of β-trans-4-bromo-cinnamic acid crystal. To a 500 mL pyrex conical flask, 400 mL DI water was added and stirred vigorously with a stir bar. The collected crystal was suspended in the DI water. The suspension was irradiated with 365nm UV light for overnight to obtain a cloudy suspension, which was filtrated afterwards to obtained 8 g of white powder. ^{1}H NMR confirmed the white powder was β-truxinic acid (**1a**). ^{1}H NMR (500 MHz, DMSO-d6): δ 12.48 (s, 2H), 7.13-7.29 (d, J = 8.5 Hz, 4H), 7.03-7.01 (d, J = 8.5 Hz, 4H), 4.20-4.19 (m, 2H), 3.79-3.78 (m, 2H). ^{13}C NMR (125 MHz, DMSO-d6): δ 173.75, 138.63, 130.68, 130.16, 119.23, 43.73, 42.36. HRMS-ESI (m/z): $[M + H]^+$ calculated for $C_{18}H_{14}Br_2O_4$, 452.9932; observed 452.9319.

Synthesis of 1b. To a 250 mL round bottom flask (RBF), compound **1a** (5 g, 11 mmol) was mixed with 100 mL acetonitrile. DIC (7 mL, 44 mmol) was added dropwise. The solid first dissolved, and then the solution became cloudy again. DMAP (380 mg, 17 mmol) and 1-undecanol (9.15 mL, 44 mmol) were then added to the solution. The reaction was stirred at r.t. for overnight. After the reaction completed, the solution was filtrated to obtain a yellow solution. The yellow solution was concentrated using rotary evaporator and diluted with 200 mL DCM. The solution was washed with DI water (100 mL×2) and brine (100mL×1). DCM phase was collected and dried with Na_2SO_4. After filtration, the solution was concentrated onto silica. Column chromatography (SiO_2, 0 ~ 10% EtOAC / hexane gradient eluent) gave compound **1b** as a colorless oil (8 g). ^{1}H NMR (500 MHz, $CDCl_3$): δ 7.27-7.25 (d, J = 8.5 Hz, 4H), 6.80-6.78 (d, J = 8.5 Hz, 4H), 4.34 – 4.29 (m, 2H), 4.12 (m, 4H), 3.75 – 3.70 (m, 2H), 1.65-1.59 (m, 4H), 1.13-1.23 (m, 32H), 0.89-0.87 (t, J = 6.9 Hz, 6H). HRMS-ESI (m/z): $[M + H]^+$ calculated for $C_{40}H_{58}Br_2O_4$, 761.2775; observed 761.2767.

Synthesis of 1c. To a 250 mL RBF, compound 1b (7 g, 9.2 mmol), $(Bpin)_2$ (5.13 g, 20.2 mmol), $Pd(dppf)Cl_2$·DCM (750 mg, 0.92 mmol), KOAc (6 g, 55 mmol) were mixed with 60 mL anhydrous DMSO. The mixture was sparged with N_2 for 10 minutes and heated up to 110 °C. The solids completely dissolved when the temperature reached ~70°C, and the solution became dark purple. The reaction was stirred at 110 °C for overnight. After the reaction completed, the solution was cooled down to r.t. and diluted with DCM (300 mL). The dilute solution was filtered with Celite®. The filtrate was washed DI water (200 mL× 3) and brine (200 mL×1). DCM phase was collected and dried with Na_2SO_4. After filtration, the solution was concentrated onto silica. Column chromatography (SiO_2, 0 ~ 25% EtOAC / hexane gradient eluent) gave a mixture of compound **1c** and monofunctionalized product as blueish solid (5 g). ^{1}H NMR suggest

the major product was compound **1c**. This mixture was used in next step without further purification. ^{1}H NMR (500 MHz, $CDCl_3$): δ 7.54 - 7.52 (d, J = 7.6 Hz, 4H), 6.95 - 6.93 (d, J = 7.6 Hz, 4H), 4.41 - 4.39 (m, 2H), 4.14 - 4.09 (m, 4H), 3.82 - 3.80 (m, 2H), 1.64 - 1.60 (m, 4H), 1.30 (m, 24H), 1.26 (m, 32H), 0.89 - 0.87 (t, J = 6.9 Hz, 6H).

Synthesis of 1d. To a 250 mL RBF, the crude compound **1c** (5g) obtained in last step and acetic acid (5.5 mL) were dissolved in 120 mL THF. The solution was cooled down in ice water bath. 30% H_2O_2 (12 mL) was added dropwise. The reaction was stirred at r.t for overnight. After the reaction completed, sodium metabisulfite (6.6 g) was added. The solution was concentrated with rotary evaporator and diluted with EtOAc (200 mL). The solution was washed with DI water (100 mL×2) and brine (100mL×1). EtOAc phase was collected and dried with Na_2SO_4. After filtration, the solution was concentrated onto silica. Column chromatography (SiO_2, 0 ~ 40% EtOAC in hexane, gradient eluent, RediSep Rf Gold Silica Flash Chromatography Column, Teledyne ISCO) gave compound **1d** as a colorless sticky oil (3.5 g). The product turned solid under vacuum. Note that compound **1d** should be stored in the freezer (side products were found by NMR after stored at r.t. for a week). ^{1}H NMR (500 MHz, $CDCl_3$): δ 6.75 - 6.74 (d, J = 8.0 Hz, 4H), 6.57 - 6.56 (d, J = 7.9 Hz, 4H), 5.35 - 5.15 (br, 2H), 4.25 - 4.24 (m, 2H), 4.15 - 4.08 (m, 4H), 3.72 - 3.71 (m, 2H), 1.64 - 1.61 (m, 4H), 1.40 - 1.17 (m, 32H), 0.89 - 0.87 (t, J = 6.8 Hz, 6H). ^{13}C NMR (125 MHz, $CDCl_3$): δ 172.84, 153.91, 130.74, 128.93, 114.85, 65.25, 44.25, 43.61, 31.80, 29.50, 29.49, 29.42, 29.23, 29.17, 28.45, 25.78, 22.57, 13.99. HRMS-ESI (m/z): $[M + H]^+$ calculated for $C_{40}H_{60}O_6$, 637.4463; observed 637.4465.

Synthesis of 1. To a 250 mL round bottom flask (RBF), compound **1d** (3.5 g, 5.5 mmol), 4-Pentynoic acid (1.13 g, 11.5 mmol) and DMAP (0.67 g, 5.5 mmol) were dissolved with 70 mL DCM. DIC (2.6 mL, 16.5 mmol) was added dropwise. The reaction was stirred at r.t. for overnight. After the reaction completed, the solution was filtrated and diluted with 50 mL DCM. The solution was washed with DI water (100 mL×2) and brine (100mL×1). DCM phase was collected and dried with Na_2SO_4. After filtration, the solution was concentrated onto silica. Column chromatography (SiO_2, 0 ~ 25% EtOAC in hexane, gradient eluent) gave compound **1** as a colorless oil (2 g). ^{1}H NMR (400 MHz, $CDCl_3$): δ 6.93 - 6.91 (d, J = 8.7 Hz, 4H), 6.88 – 6.87 (d, J = 8.7 Hz, 4H), 4.38 - 4.37 (m, 2H), 4.18 - 4.07 (m, 4H), 3.77 – 3.74 (m, 2H), 2.76 – 2.73 (t, J = 7.4 Hz, 4H), 2.60 – 2.57 (td, J = 7.4, 2.6 Hz, 4H), 2.01 (t, J = 2.6 Hz, 2H), 1.66 – 1.57 (m, 4H), 1.36 – 1.26 (m, 32H), 0.89 – 0.87 (t, J = 6.9 Hz, 6H). ^{13}C NMR (100 MHz, $CDCl_3$): δ 172.64, 170.50, 149.44, 136.70, 129.20, 121.52, 82.44, 69.80, 65.75, 44.75, 44.07, 33.84, 32.32, 30.01, 29.94, 29.74, 29.69, 28.98, 26.30, 23.08, 14.79, 14.51. HRMS-ESI (m/z): $[M + H]^+$ calculated for $C_{50}H_{68}O_8$, 798.09; observed 797.4984.

2. Synthesis of linker 2 and polymer PII that contains mechanophore II with stored length

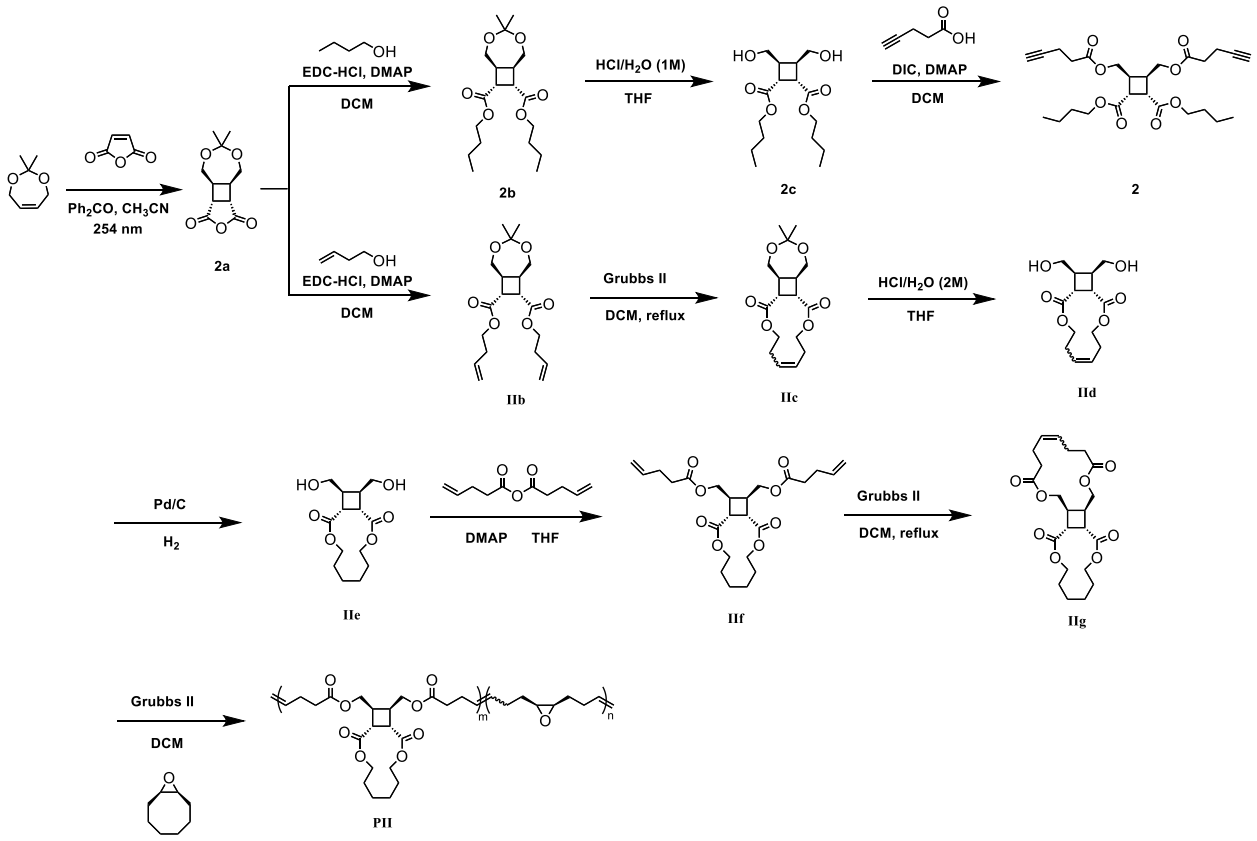

Scheme S2. Synthetic route of linker **2**, bis-alkene Mechanophore **II** with stored length, and polymer **PII**.

Synthesis of linker 2

Synthesis of 2a and 2b. 2,2-Dimethyl-1,3-dioxep-5-ene (14 g, 109 mmol, 1 eq.), prepared according to literature precedent,[9] was charged to a 1 L quartz round bottom flask equipped with a magnetic stir bar along with maleic anhydride (11.8 g, 11.9 mmol, 1.1 eq.) and benzophenone (5.5 g). Then, 550 mL of acetonitrile was added to dissolve all components and the colorless solution was sparged with N_2 (g) for 10 minutes. Then, the N_2 (g) inlet was removed and the sealed reaction flask was placed in a Rayonet photoreaction chamber and irradiated with UV light (254nm) for 50 hours with stirring. After the reaction completed, the solution was concentrated obtain crude product of **2a**. ^{1}H NMR suggest the crude product mainly contain benzophenone, maleic anhydride and **2a**. To a 500 mL flask, crude product of **2a** (31 g) and 1-butanol (24.7 mL, 270 mmol) were dissolved with 120 mL DCM. DMAP (1.1 g, 9 mmol) was then added to the solution. The solution turned dark brown in a few seconds. EDC·HCl (34 g, 177 mmol) was then added portion-wise. The reaction was stirred at r.t. for overnight. After the reaction completed, the solution

was diluted with 100 mL DCM and washed with DI water (120 mL×2) and brine (100 mL×1). DCM phase was then dried with Na_2SO_4. After filtration, the dark brown solution was then concentrated onto silica. Note that compound **2b** cannot be visualized on TLC with $KMnO_4$ stain. The eluent was chosen based on previous literature with similar structure.[9] Column chromatography (SiO_2, 0~25% EtOAC in hexane, gradient eluent) gave compound **2b** with some impurities as a yellowish liquid (3.2 g). The produce was used in next step without further purification. ^{1}H NMR (500 MHz, $CDCl_3$): δ 4.07 – 4.04 (m, 4H), 3.87 – 3.84 (m, 2H), 3.72 – 3.69 (m, 2H), 3.24 – 3.21 (br, 2H), 2.86 – 2.83 (br, 2H), 1.60 – 1.54 (m, 4H), 1.38 – 1.31 (m, 10H), 0.92 – 0.89 (t, J = 7.4 Hz, 6H).

Synthesis of 2c. To a 1 L RBF, compound **2b** (3.2 g, 9 mmol) was dissolved in 250 mL of THF and cooled to 0 °C in an ice-water bath. Then, 125 mL of a 1 M HCl solution was added dropwise. The reaction was stirred for 3 hours at 0 °C and then quenched by the dropwise addition of saturated $NaHCO_3$ (aq) until a pH of 7 was achieved. The solution was concentrated with rotary evaporator and washed with ethyl acetate (100 mL × 2). The combined organic layers were washed with brine (100 mL × 1) and subsequently dried over Na_2SO_4. Purification by flash chromatography (SiO_2, 0 ~ 75% EtOAC in hexane, gradient eluent) furnished compounds **2c** as colorless oil (2.5 g). ^{1}H NMR (500 MHz, DMSO-d6): δ 4.63 (br, 2H), 3.98 – 3.95 (t, J = 6.6 Hz, 4H), 3.60 – 3.57 (br, 2H), 3.53 – 3.50 (br, 2H) 3.14 – 3.13 (d, J = 5.1 Hz, 2H), 2.69 (br, 2H), 1.54 – 1.48 (m, 4H), 1.35 – 1.27 (m, 4H), 0.89 – 0.86 (t, J = 7.4 Hz, 6H). ^{13}C NMR (125 MHz, DMSO-d6): δ 172.55, 63.64, 59.86, 40.25, 39.00, 30.15, 18.59, 13.54. HRMS-ESI (m/z): $[M + H]^+$ calculated for $C_{16}H_{28}O_6$, 317.1959; observed 317.1968.

Synthesis of 2. To a 100 mL RBF, compound **1d** (7.87 g, 7.5 mmol), 4-Pentynoic acid (1.55 g, 15.8 mmol) and DMAP (0.92 g, 7.5 mmol) were dissolved with 50 mL DCM. DIC (2.5 mL, 15.8 mmol) was added dropwise. The reaction was stirred at r.t. for overnight. After the reaction completed, the solution was filtrated and diluted with 50 mL DCM. The solution was washed with DI water (100 mL×2) and brine (100mL × 1). DCM phase was collected and dried with Na_2SO_4. After filtration, the solution was concentrated onto silica. Column chromatography (SiO_2, 0 ~ 33% EtOAC in hexane, gradient eluent) gave linker **2** as a colorless oil (2.4 g). ^{1}H NMR (500 MHz, $CDCl_3$): δ 4.27 – 4.26 (m, 4H), 4.10 – 4.02 (m, 4H), 3.24 – 3.23 (m, 2H), 3.15 – 3.13 (m, 2H), 2.57 – 2.54 (m, 4H), 2.50 – 2.47 (m, 4H), 1.98 – 1.97 (t, J = 2.6 Hz, 2H), 1.61 – 1.55 (m, 4H), 1.39 – 1.31 (m, 4H), 0.93 – 0.90 (t, J = 7.4 Hz, 6H). ^{13}C NMR (125 MHz, CDCl3): δ 172.01, 171.60, 82.37, 69.40, 65.02, 63.55, 41.23, 36.16, 33.42, 30.68, 19.20, 14.45, 13.80. HRMS-ESI (m/z): $[M + H]^+$ calculated for $C_{26}H_{36}O_8$, 477.2483; observed 477.2484.

Synthesis of polymer PII that contains mechanophore II with stored length

Synthesis of IIb. 2,2-Dimethyl-1,3-dioxep-5-ene (2.56 g, 20 mmol, 1 eq.), prepared according to literature precedent,[9] was charged to a 250 mL quartz round bottom flask equipped with a magnetic stir bar along with maleic anhydride (4.31g, 20 mmol, 2.2 eq.) and benzophenone (1 g). Then, 100 mL of acetonitrile was added to dissolve all components and the colorless solution was sparged with N_2 (g) for 30 minutes. Then, the N_2 (g) inlet was removed and the sealed reaction flask was placed in a Rayonet photoreaction chamber and irradiated with UV light (254nm) for 50 hours with stirring. Then, the reaction was removed from the chamber and DMAP (0.54 g, 4.4 mmol, 0.2 eq.), EDC (16.8 g, 88 mmol, 4.4 eq.), and the corresponding alcohol (132 mmol, 6.6 eq.) were added to the reaction flask. The reaction was allowed to stir at room temperature overnight under ambient conditions. The solvent was then evaporated under reduced pressure and the remaining brown sludge was dissolved in 200 mL of ethyl acetate. The solution was washed with water (200 mL × 3) and brine (200 mL). The organic solution was then dried over Na_2SO_4. Solvent was removed under reduced pressure and purification by flash chromatography (SiO_2, 0 ~ 10% EtOAC in hexane, gradient eluent) furnished the desired product as a colorless oil with an isolated yield of 10%. ^{1}H NMR (500 MHz, $CDCl_3$): δ 5.77 (ddt, J = 17.0, 10.3, 6.7 Hz, 2H), 5.15 – 5.03 (m, 4H), 4.19 – 4.06 (m, 4H), 3.86 (dt, J = 13.1, 2.4 Hz, 2H), 3.75 – 3.67 (m, 2H), 3.24 (s, 2H), 2.85 (s, 2H), 2.37 (qt, J = 6.8, 1.4 Hz, 4H), 1.38 – 1.37 (m, 6H). ^{13}C NMR (125 MHz, $CDCl_3$): δ 172.65, 133.84, 117.27, 117.22, 63.86, 61.41, 40.04, 39.42, 32.95, 30.91. HRMS-ESI (m/z): $[M + H]^+$ calculated for $C_{19}H_{28}O_6$, 353.1959; found, 353.1952.

Synthesis of IIc. A solution of Grubbs catalyst 2nd generation (0.2 mmol, 0.1 eq.) in 1000 mL dichloromethane was sparged with N_2 (g) for 30 minutes while stirring. To this solution was added dropwise a solution of **IIb** (2 mmol, 1 eq.) in 5 mL of dichloromethane and the reaction was heated to 40 °C until disappearance of the starting material was observed by TLC. The reaction was cooled to room temperature, then opened to atmosphere and quenched with 3 mL of ethyl vinyl ether. Purification by flash chromatography (SiO_2, 0 ~ 30% EtOAC in hexane, gradient eluent) furnished **IIc** as white solid with an isolated yield of 70%. ^{1}H NMR (500 MHz, $CDCl_3$): δ 5.54 – 5.34 (m, 2H), 4.46 – 4.41 (m, 2H), 4.10 – 3.96 (m, 2H), 3.87 – 3.84 (m, 2H), 3.72 – 3.67 (m, 2H), 3.24 (s, 2H), 2.90 (d, J = 19.0 Hz, 2H), 2.57 – 2.25 (m, 4H), 1.39 – 1.32 (m, 6H). ^{13}C NMR (125 MHz, $CDCl_3$): δ 172.38, 172.25, 128.95, 128.57, 102.42, 63.52, 62.64, 61.84, 61.80, 40.68, 40.34, 39.04, 38.70, 31.98, 27.25, 25.40, 23.69. HRMS-ESI (m/z): $[M + Na]^+$ calcd for $C_{17}H_{24}O_6$, 347.1465; found, 347.1467.

Synthesis of IId. Compound **IIc** (0.85 mmol) was dissolved in 25 mL of THF and cooled to 0 °C in an ice-water bath. Then, 12.5 mL of a 2M HCl solution was added dropwise. The reaction was stirred for 1 hour

at 0 °C and then quenched by the dropwise addition of saturated $NaHCO_3$ (aq) until a pH of 7 was achieved. The solution was then allowed to warm to room temperature and was extracted with ethyl acetate (100 mL × 2). The combined organic layers were washed with brine and subsequently dried over Na_2SO_4. Purification by flash chromatography (SiO_2, 0 ~ 70% EtOAC in hexane, gradient eluent) furnished compounds **IId** as white solid with an isolated yield of 60%. ^{1}H NMR (500 MHz, $CDCl_3$): δ 5.57 – 5.34 (m, 2H), 4.47 – 4.41 (m, 2H), 4.10 – 3.96 (m, 2H), 3.84 – 3.77 (m, 4H), 3.24 – 3.16 (m, 2H), 3.11 – 2.92 (m, 4H), 2.60 – 2.24 (m, 4H). ^{13}C NMR (125 MHz, $CDCl_3$): δ 172.66, 172.47, 128.92, 128.55, 63.73, 62.91, 61.43, 61.40, 40.62, 40.42, 39.42, 39.07, 31.74, 27.23. HRMS-ESI (m/z): $[M + H]^+$ calculated for $C_{14}H_{20}O_6$, 285.1333; found, 285.1337.

Synthesis of IIe. Diol **IId** (1 mmol) was dissolved in 10 mL of dry methanol in a 25 mL flame-dried, 2-neck round bottom flask and sparged with Ar (g) for 15 minutes. Then, 2 mg of palladium on carbon (10 wt. % loading) was added and the suspension was further sparged with Ar (g) for 15 minutes. The suspension was then placed under vacuum for 10 seconds and backfilled with H_2 (g) via balloon. The suspension was then sparged with H_2(g) for 6 hours. Then, the outlet needle was removed, and the suspension was allowed to stir overnight under an atmosphere of H_2(g). The hydrogen balloon was then removed, and the suspension was sparged with Ar(g) for 10 minutes and then poured over Celite® and washed with MeOH (100 mL). Purification by flash chromatography (SiO_2, 0 ~ 30% EtOAC in hexane, gradient eluent) furnished compounds **IIe** as white solid with an isolated yield of 65%. ^{1}H NMR (500 MHz, $CDCl_3$): δ 4.45 – 4.41 (m, 2H), 4.03 – 3.94 (m, 2H), 3.85 – 3.79 (m, 4H), 3.29 – 3.21 (m, 2H), 3.13 – 2.92 (m, 4H), 1.73 – 1.50 (m, 8H), 1.48 – 1.36 (m, 2H). ^{13}C NMR (125 MHz, $CDCl_3$): δ 172.87, 65.04, 61.35, 40.61, 38.96, 26.31, 24.32.

Synthesis of IIf. Compound **IIe** (1 mmol, 1 eq.) and 4-dimethylaminopyridine (1.8 mmol, 1.8 equivalent) were dissolved in anhydrous THF (10 mL) in a 20 mL scintillation vial. Under an atmosphere of N_2 (g), 4-pentenoic anhydride (4.4 mmol, 4.4 eq.) was added dropwise via syringe and the reaction was stirred at room temperature overnight. Excess anhydride was quenched with 1 mL MeOH. Purification by flash chromatography (SiO_2, 0 ~ 20% EtOAC in hexane, gradient eluent) furnished compounds **IIf** as colorless oil with yield of 60%. ^{1}H NMR (500 MHz, $CDCl_3$): δ 5.85 – 5.78 (m, 2H), 5.10 – 4.97 (m, 4H), 4.50 – 4.39 (m, 2H), 4.27 – 4.16 (m, 4H), 3.99 – 3.95 (m, 2H), 3.30 – 3.15 (m, 4H), 2.43 – 2.33 (m, 8H), 1.69 – 1.65 (m, 4H), 1.61 – 1.53 (m, 4H), 1.45 – 1.37 (m, 2H). ^{13}C NMR (125 MHz, CDCl3): δ 172.76, 171.81, 136.47, 115.65, 65.14, 63.08, 41.63, 35.59, 33.42, 28.72, 26.37, 24.30. HRMS-ESI (m/z): $[M + H]^+$ calculated for $C_{24}H_{34}O_8$, 451.2326; found, 451.2335.

Synthesis of IIg. An identical procedure to that of compounds **IIc** was followed, yielding compounds **IIg** as white solids with a yield of 70%. ^{1}H NMR (500 MHz, CDCl3): δ 5.47 – 5.54 (m, 2H), 4.48 – 4.43 (m,

2H), 4.27 – 4.16 (m, 4H), 4.03 – 3.94 (m, 2H), 3.30 – 3.16 (m, 4H), 2.37 – 2.23 (m, 8H), 1.70 – 1.66 (m, 4H), 1.61 – 1.53 (m, 4H), 1.45 – 1.39 (m, 2H). ^{13}C NMR (125 MHz, $CDCl_3$): δ 173.24, 171.89, 130.36, 65.22, 63.57, 40.02, 35.94, 34.56, 27.70, 26.29, 24.31. HRMS-ESI (m/z): $[M + H]^+$ calculated for $C_{22}H_{30}O_8$, 432.2013; found, 432.2015.

Polymerization of IIg to obtain polymer PII. A 2 mL crimp top vial was charged with **IIg** and freshly distilled 9-oxabicyclo[6.1.0]non-4-ene under N_2 (g). A stock solution of Grubbs Catalyst 2nd Generation in dry DCM was prepared and sparged with N_2 (g) for 15 min. Then, the Grubbs Catalyst solution (0.00067 equiv.) was added via air-tight syringe to dissolve the monomers and initiate the polymerization. After 16 hours, the polymerization was quenched with 10 drops of ethyl vinyl ether and then precipitated into methanol to give the crude polymer. Polymers were purified via one additional precipitation into MeOH and one reverse precipitation from DCM according to literature precedent.[10] The polymer was dried on the high vac for at least 1 hour prior to use. ^{1}H NMR (500 MHz, CDCl3): δ 5.54 – 5.35 (m, 2H), 4.45 – 4.41 (m, 0.54H), 4.24 – 4.15 (m, 1.07H), 3.97 – 3.93 (m, 0.54H), 3.28 – 3.25 (m, 0.55H), 3.19 – 3.16 (m, 0.54H), 2.92 – 2.89 (m 1.41H), 2.39 – 2.06 (m, 5.15H), 1.69 – 1.47 (m, 4.87H), 1.46 – 1.18 (m, 4.75H). ^{1}H NMR indicates that there were 27% mechanophore **II** and 73% epoxide. GPC: M_n = 245 kDa, M_w = 329 kDa, PDI = 1.3.

3. Synthesis of linker 3

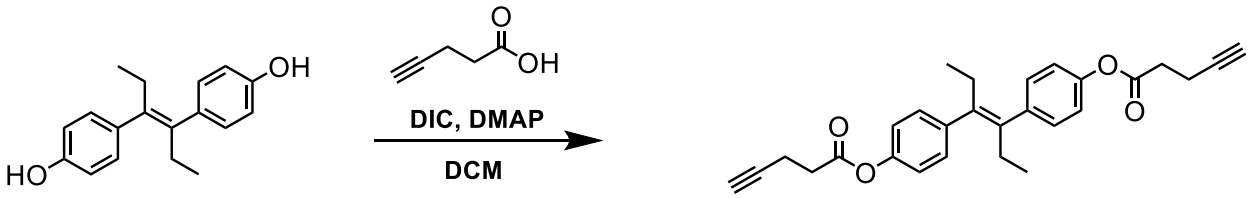

3

Scheme S3. Synthetic scheme of linker **3**.

To a 50 mL RBF, diethylstilbestrol (1 g, 3.7 mmol), 4-Pentynoic acid (0.77 g, 7.8 mmol) and DMAP (0.46 g, 3.7 mmol) were dissolved with 20 mL DCM. DIC (1.75 mL, 11.1 mmol) was added dropwise. The reaction was stirred at r.t. for overnight. After the reaction completed, the solution was filtrated and diluted with 20 mL DCM. The solution was washed with DI water (25 mL×2) and brine (25 mL×1). DCM phase was collected and dried with Na_2SO_4. After filtration, the solution was concentrated onto silica. Column chromatography (SiO_2, 0 ~ 33% EtOAC in hexane, gradient eluent) gave linker **3** as a white solid (0.65 g).

^{1}H NMR (500 MHz, $CDCl_3$): 7.21 – 7.19 (d, J = 8.4 Hz, 4H), 7.11 – 7.10 (d, J = 8.5 Hz, 4H), 2.84 – 2.82 (t, J = 7.3 Hz, 4H), 2.67 – 2.64 (m, 4H), 2.14 – 2.10 (q, J = 7.4 Hz, 4H), 2.06 – 2.04 (t, J = 2.6 Hz, 2H), 0.78 – 0.75 (t, J = 7.4 Hz, 6H). ^{13}C NMR (125 MHz, $CDCl_3$) δ 170.77, 149.45, 140.46, 139.27, 130.04, 121.43, 82.50, 69.82, 33.94, 28.89, 14.90, 13.65. HRMS-ESI (m/z): $[M + H]^+$ calculated for $C_{28}H_{28}O_4$, 429.53; observed 429.2061.

4. Synthesis of azide-terminated 4-arm PEG[11]

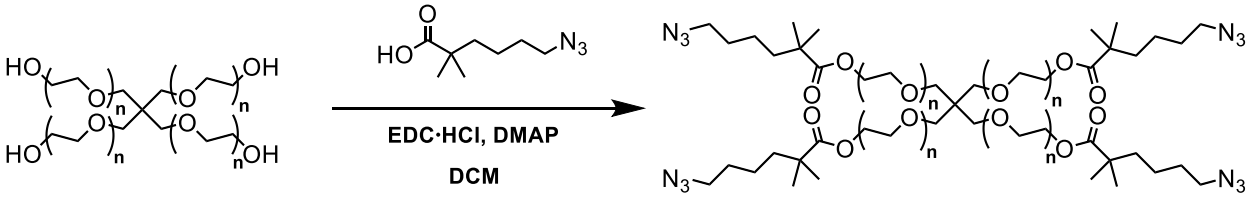

Scheme S3. Synthetic scheme of azide-terminated 4-arm PEG.

The 4-arm PEG 5000 (Creative PEGWorks, actual MW = 5108 g/mol) was dissolved in minimal ethyl acetate, precipitated by dropwise addition to a stirring beaker of cold diethyl ether, and dried for at least 12 hours in a vacuum oven before use. To a 100 mL flame-dried Schlenk flask was added 3.0 g (0.59 mmol) of 4-arm PEG , 2.25 g (11.8 mmol) EDC·HCl, 0.62 g (5.0 mmol) 4-dimethylaminopyridine, and 1.09 g (5.9 mmol) of 6-azido-2,2-dimethylhexanoic acid[11]. After addition, the flask was evacuated and refilled with nitrogen three times. The starting materials were dissolved in minimal amount of dry DCM. The reaction was stirred at r.t. for 24 hours. After the reaction completed, the solution was poured into 50 ml water and washed twice with water and twice with brine. The organic phase was dried with sodium sulfate and concentrate with rotary evaporator. After the solution became viscous, the PEG was precipitated directly by dropwise addition to a stirring beaker of cold diethyl ether and the PEG was collected on a Buchner funnel. Repeat the precipitation twice, and the final product was dried and collected as a white powder with a 79% yield (2.68 g). ^{1}H-NMR (400 MHz, $CDCl_3$) δ: 4.24 (t, 8H), 3.73-3.54 (m, 464H), 3.28 (t, 8H), 1.65-1.55 (m, 16H), 1.37-1.29 (m, 8H), 1.20 (s, 24H).

III. Gel preparation and Gel characterizations

Gel preparation. A 50 mg/ml CuBr catalyst solution for the copper catalyzed alkyne azide click chemistry (CuAAC) was prepared in propylene carbonate according to literature procedure.[12] All gels for this study were synthesized at 25 mM (~10 wt%) PEG concentration. Azide-functionalized PEG and the

corresponding stoichiometric amount of mechano-sensitive crosslinker (Linkers **1-3**) were massed into an 8 mL scintillation vial and brought into the glovebox. The solids were dissolved in propylene carbonate and vortexed (complete dissolution of the strong and weak bonds often took up to an hour). Two stoichiometric equivalents (based on reactive group) of copper solution were added via micropipette followed by vortexing. The solution was transferred to a 5.5 x 10 x 0.1 cm Teflon mold via syringe, gently tapped to release any bubbles, and left to react in the glovebox for 24 hours (although gelation typically occurred within 10 minutes).

Gel characterizations and mechanical testing

Rheology. Rheological measurements were conducted on an Anton Paar MCR 301 rheometer with a disposable 10 mm parallel plate geometry. Samples were cut to size with a 10 mm diameter biopsy punch. The plates were covered with adhesive sandpaper to prevent slipping (Norton, A275, 120 grit, Aluminum Oxide). Frequency sweep measurements were conducted at 23 °C with a constant 0.5% shear strain, well within the linear viscoelastic regime based on initial strain sweeps. Constant temperature was maintained with a Peltier temperature control stage. Three samples from different positions in the gel were punched out for shear moduli measurement. Note that the loss moduli at low frequency typically have a large degree of error due to poor instrument sensitivity.

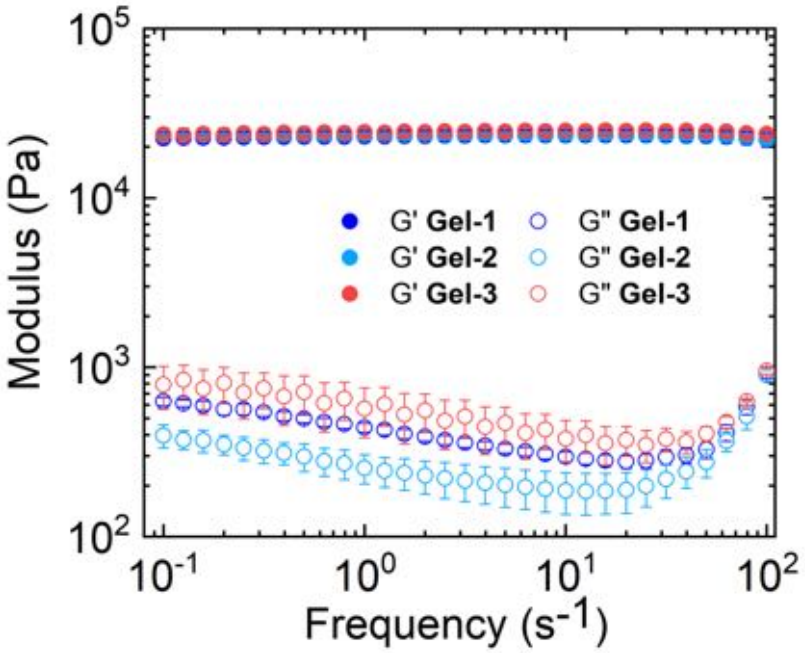

Figure S1. Frequency sweep of Gels **1-3** at the as-prepared state.

FT-IR. Fourier-transform infrared attenuated total reflectance (FTIR-ATR) spectroscopy was performed on a Bruker Alpha II FTIR spectrometer with a Diamond Crystal ATR accessory. Disappearance of the alkyne and azide IR peaks was confirmed for all of the gels synthesized.

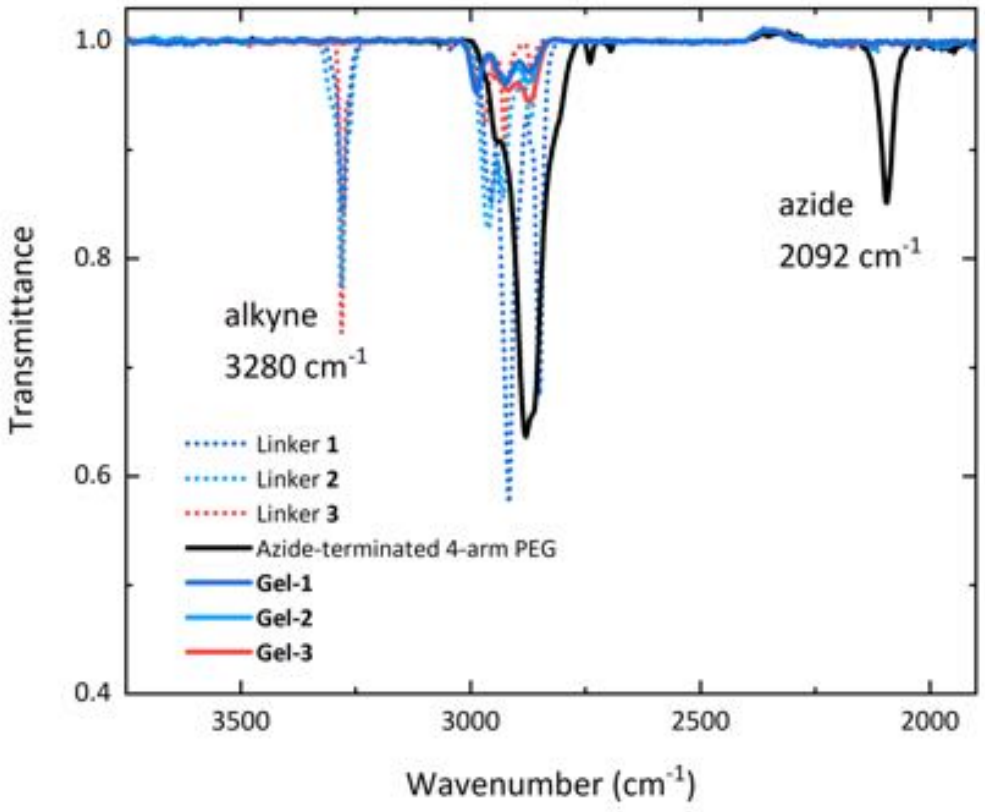

Figure S2. FTIR-ATR spectra of linkers **1-3**, azide-terminated 4-arm PEG and **Gels 1-3** show the disappearance of alkyne and azide peaks of linkers and azide-terminated 4-arm PEG.

Tearing energy. Samples for tearing energy were cut with a razor blade as a 20 x 20 mm square. This was reduced to a 20 x 4 mm area after clamping. Each measurement used 3 un-notched samples and 5 notched samples; for notched samples, a 5 mm cut was made in the center of one side of the piece, perpendicular to the edge. The exact thickness, width, and cut length were measured with calipers and a ruler before measurement. Samples were loaded into the clamps at a gauge length of ~2 mm, then stretched to a force of 0.01 N, which resulted in an initial gauge length of 4 ± 0.5 mm. Unnotched samples were pulled to 100% strain or failure (**Gel-1**) and notched samples were pulled to failure at a constant rate of 0.011 mm/s (0.66 mm/min). Tearing energy was calculated using the Thomas-Rivlin method[13] where the strain energy

is obtained by integrating the un-notched stress-strain curve to the strain at which the crack of the notched samples began to propagate.

Equilibrium swelling and sol fraction measurements. Disks for swelling were punched out with a 10 mm biopsy punch; four replicates were made for each gel. The initial mass of each disk was recorded and used to calculate the pre-gel mass of polymer. Each sample was submerged in 10 ml water and solvent exchanged every 12 hours to facilitate extraction of the copper. After the disks had equilibrated (typically after 5 solvent exchanges, based on < 1% mass change between exchanges) they were either lyophilized so the dry polymer mass could be recorded to calculate the sol fraction, or solvent exchanged with THF until equilibrated to calculate the equilibrium swelling (Figure 2c). The sol fractions were calculated to be: 0.053 ± 0.013, 0.021 ± 0.008 and 0.042 ± 0.02 for **Gel 1-3**, respectively. After equilibrium was achieved in THF, samples were dried in a vacuum oven to record the dry polymer mass.

IV. Force-extension curve of polymer PII

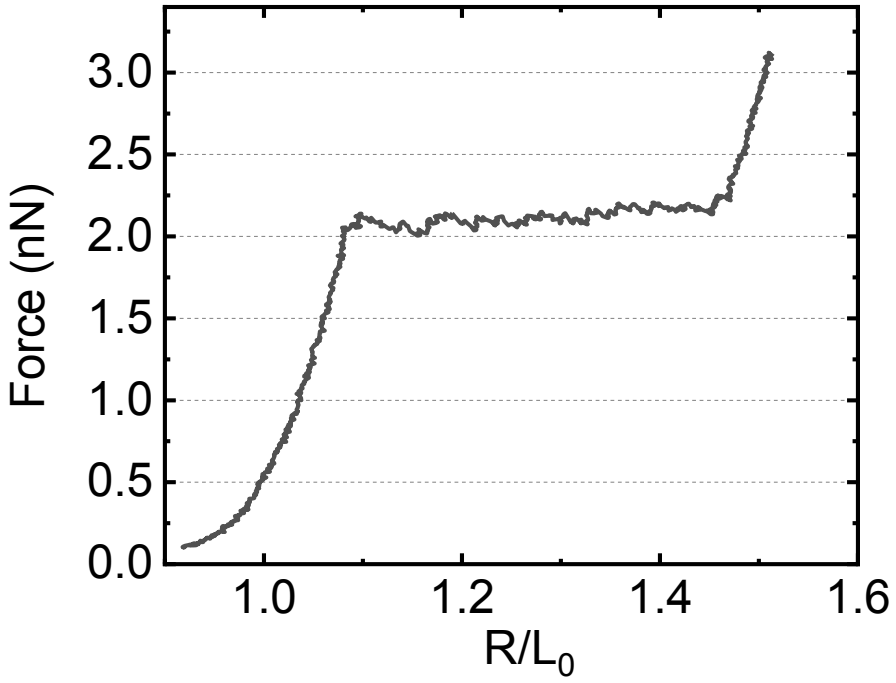

Figure S3. Representative force-extension curve for polymer **PII**. Horizontal dashed lines are the guide of force. Mechanophore II can be activated at around 2.1 ± 0.1 nN with 300 nm/s pulling rate and ~20 pN/nm spring constant of cantilever.

V. NMR spectra

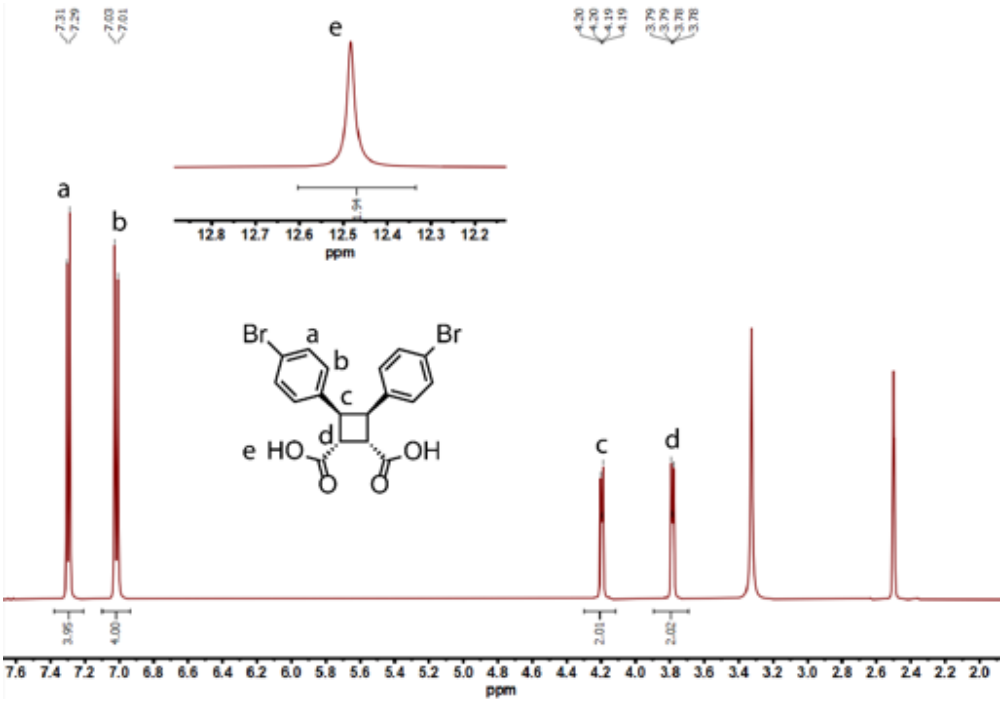

^{1}H NMR (500 MHz, DMSO-d6) spectrum of **1a**

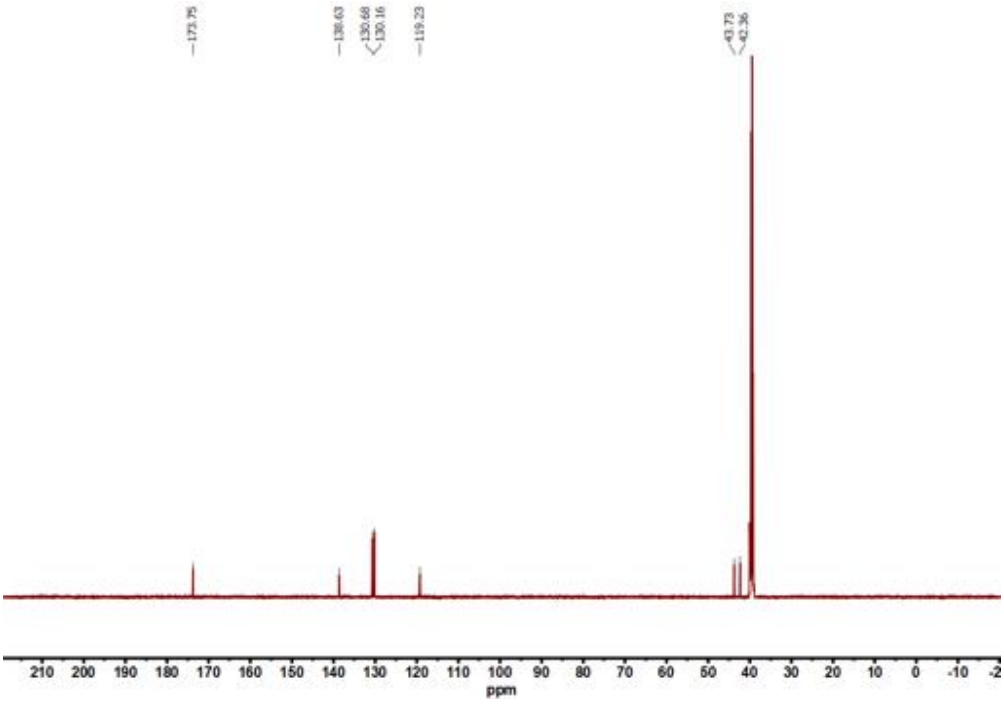

^{13}C NMR (125 MHz, DMSO-d6) spectrum of compound **1a**

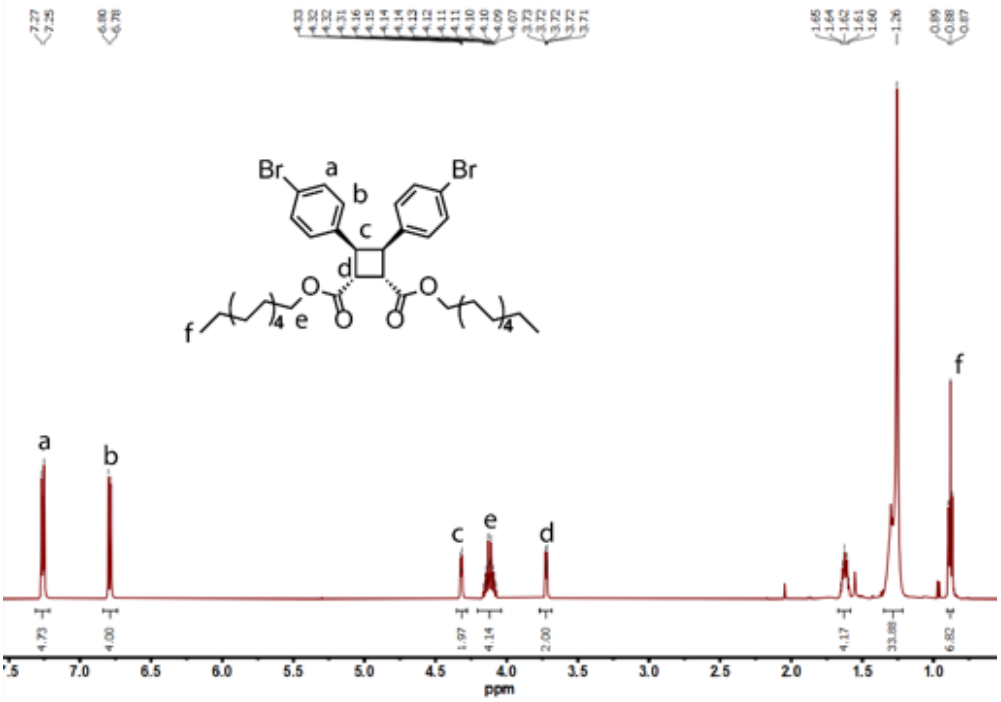

^{1}H NMR (500 MHz, $CDCl_3$) spectrum of **1b**

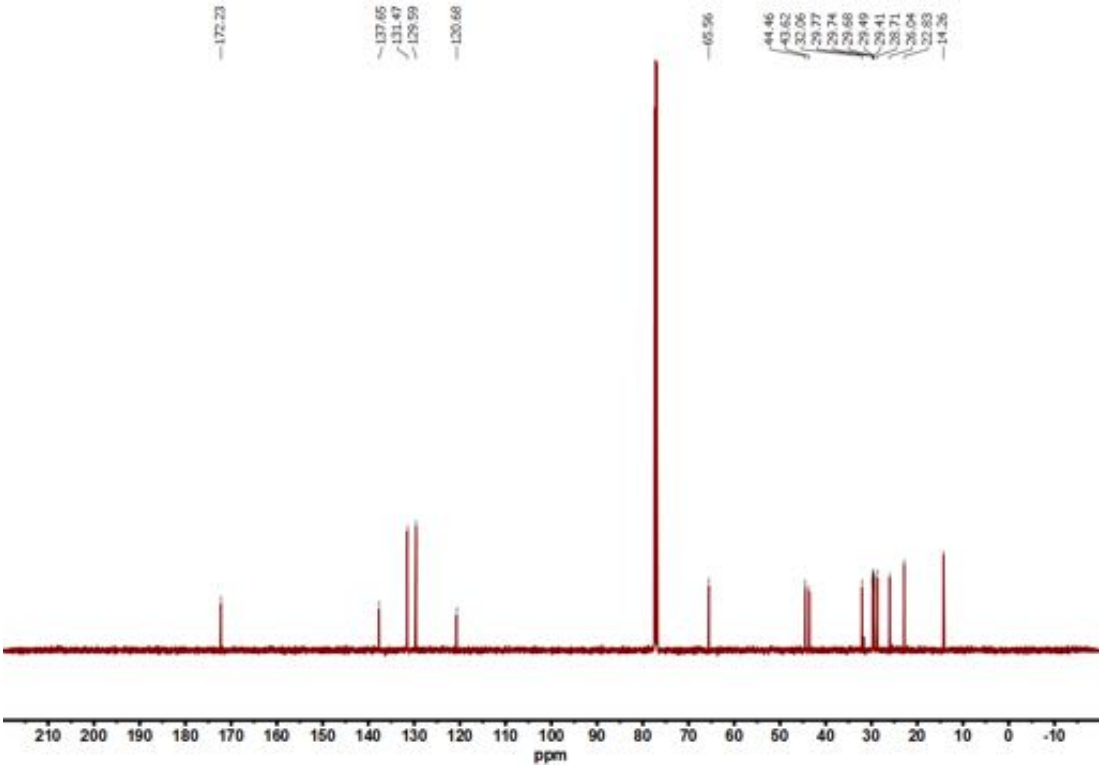

^{13}C NMR (125 MHz, $CDCl_3$) spectrum of compound **1b**

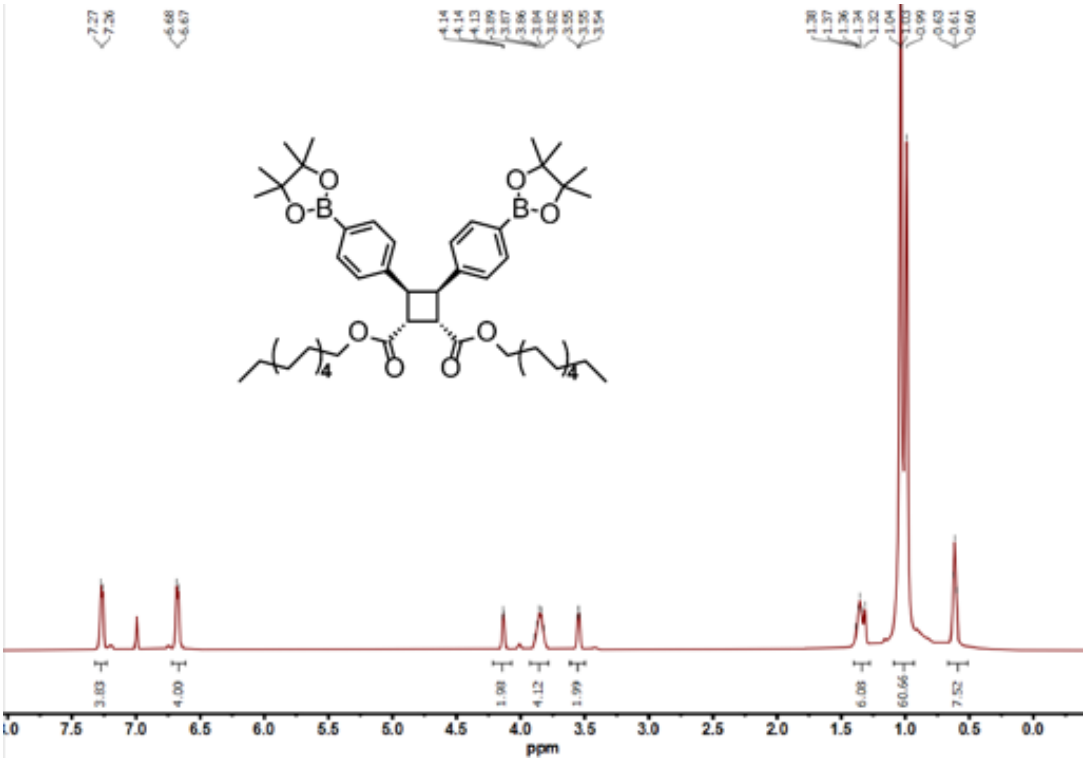

^{1}H NMR (500 MHz, $CDCl_3$) spectrum of **1c** with small amount of monofunctional byproduct.

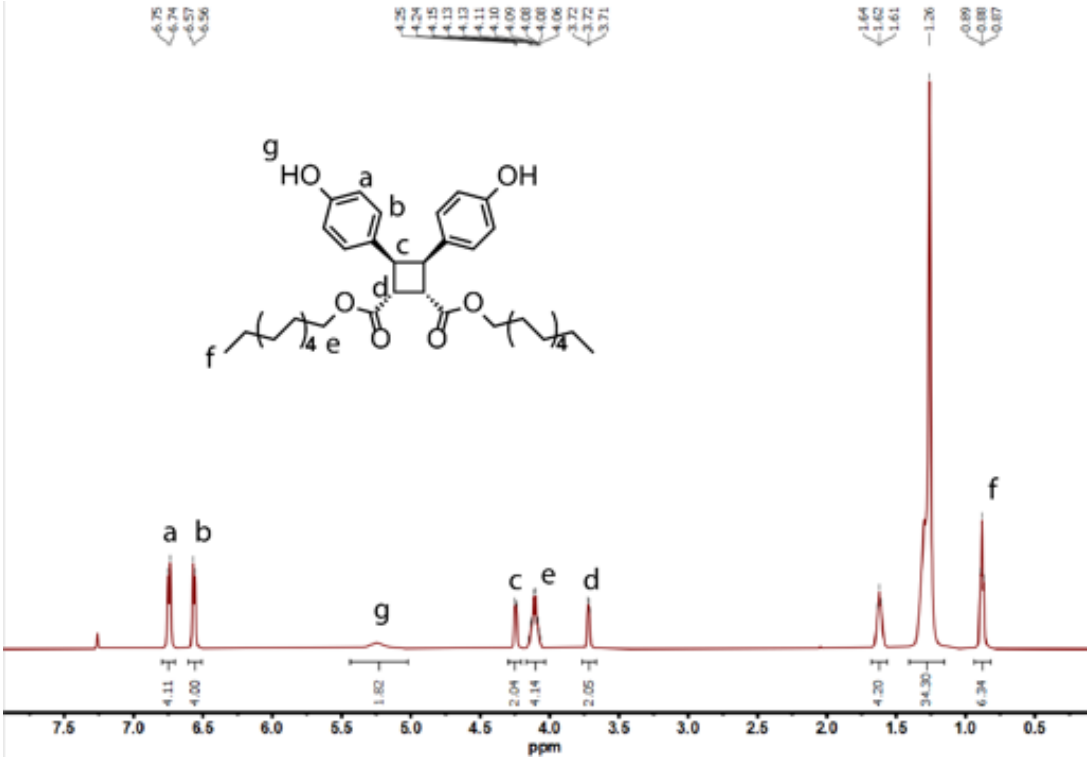

^{1}H NMR (500 MHz, $CDCl_3$) spectrum of **1d**

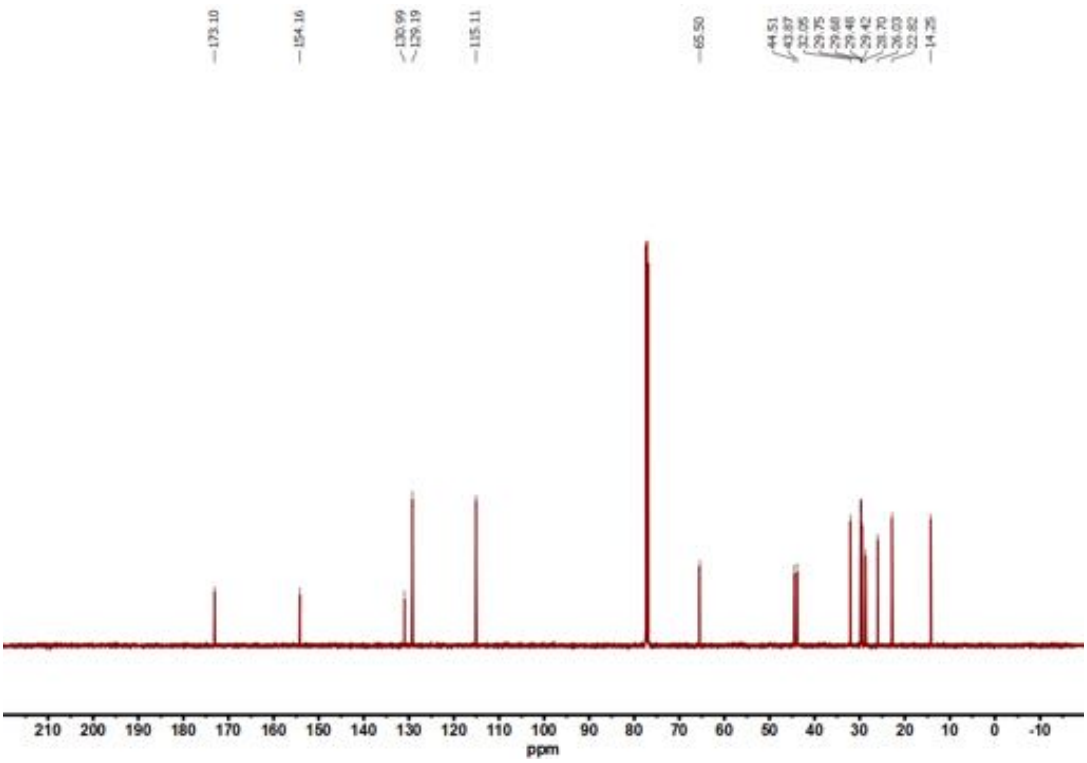

^{13}C NMR (125 MHz, $CDCl_3$) spectrum of compound **1d**

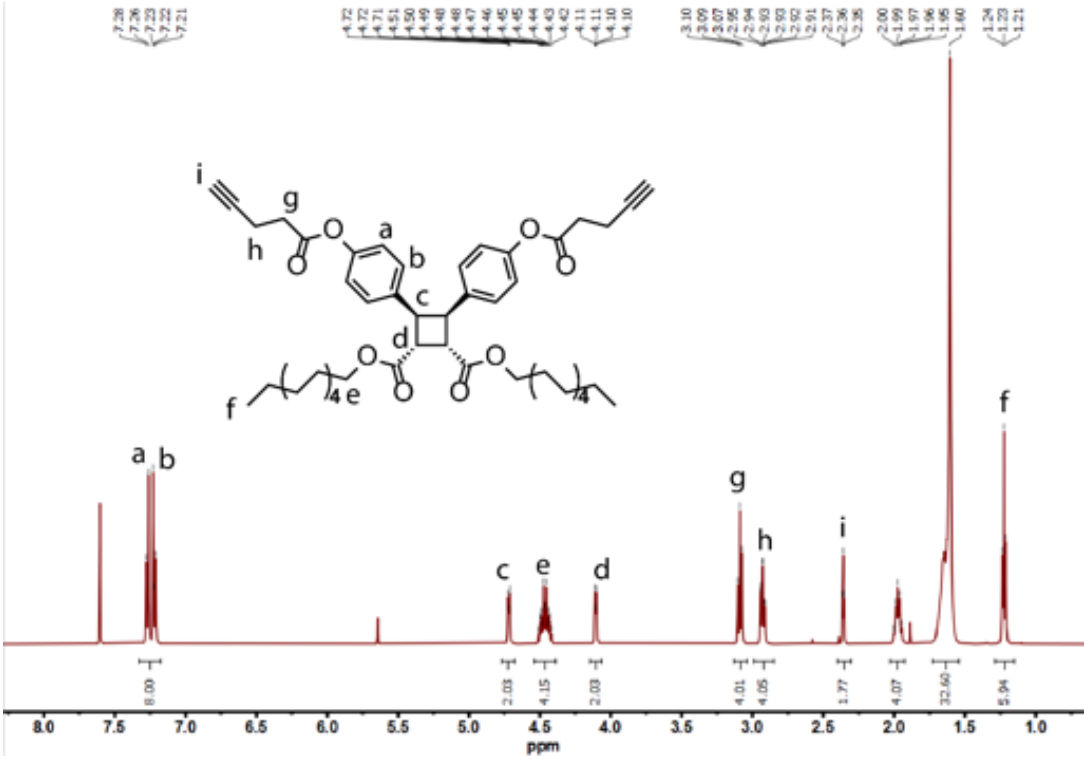

^{1}H NMR (400 MHz, $CDCl_3$) spectrum of **1**

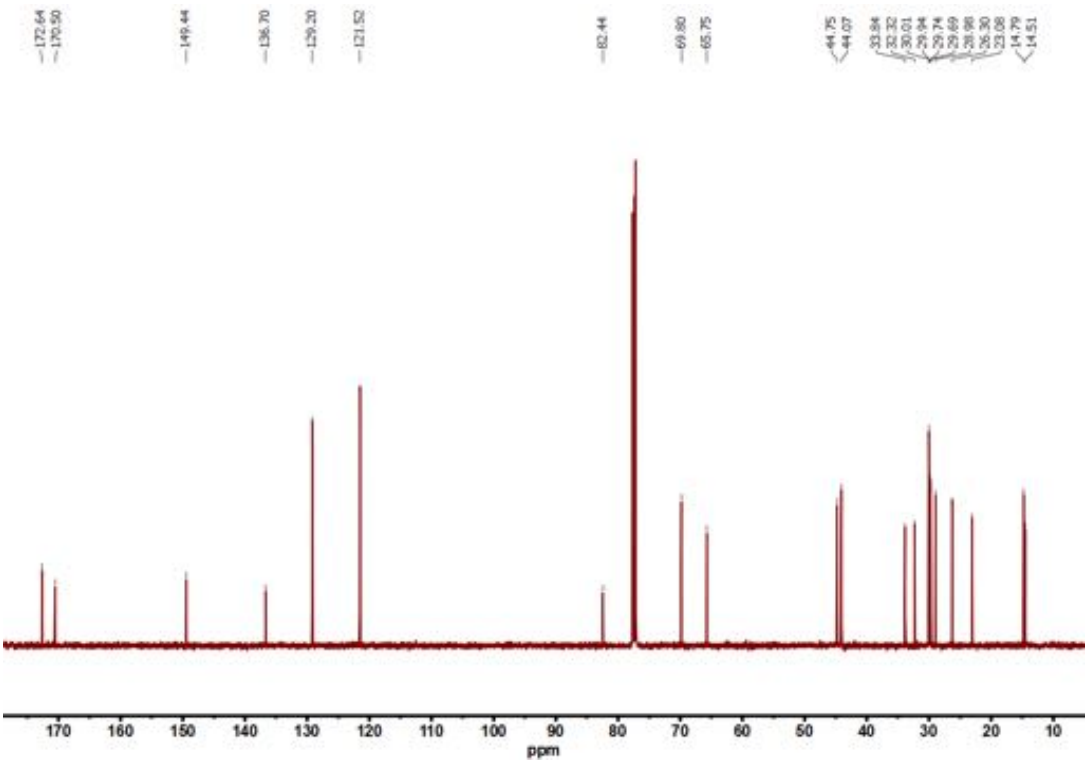

^{13}C NMR (100 MHz, $CDCl_3$) spectrum of **1**

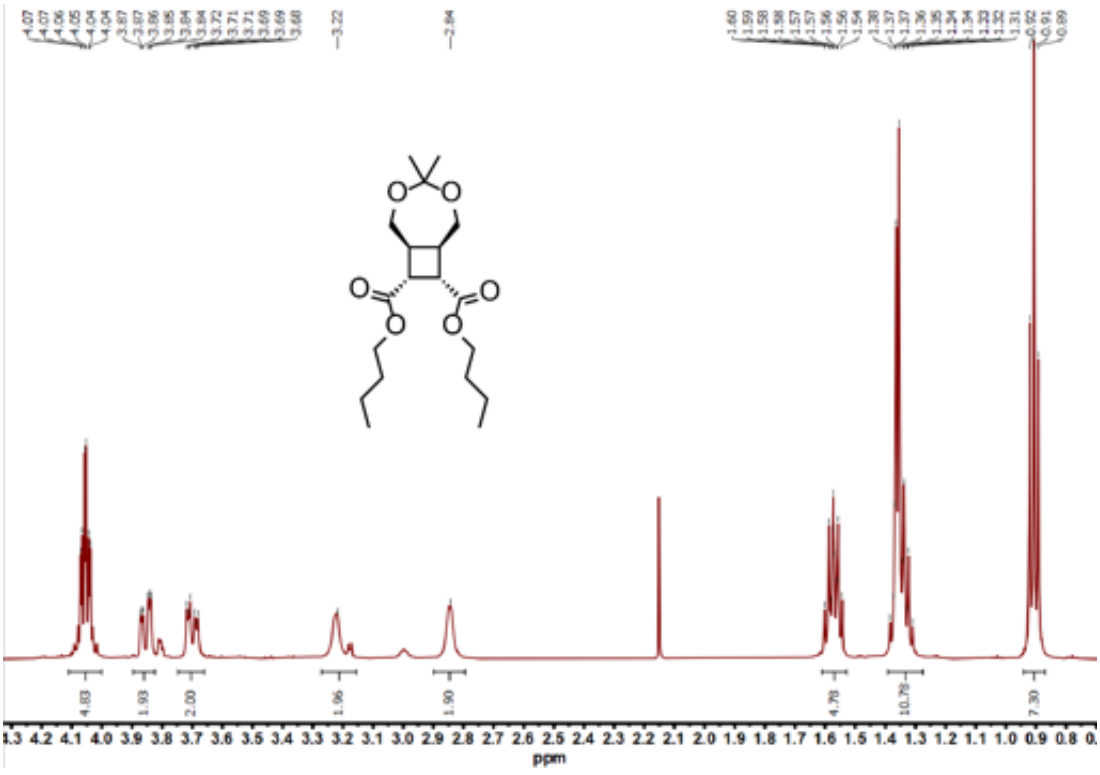

^{1}H NMR (500 MHz, $CDCl_3$) spectrum of **2b**

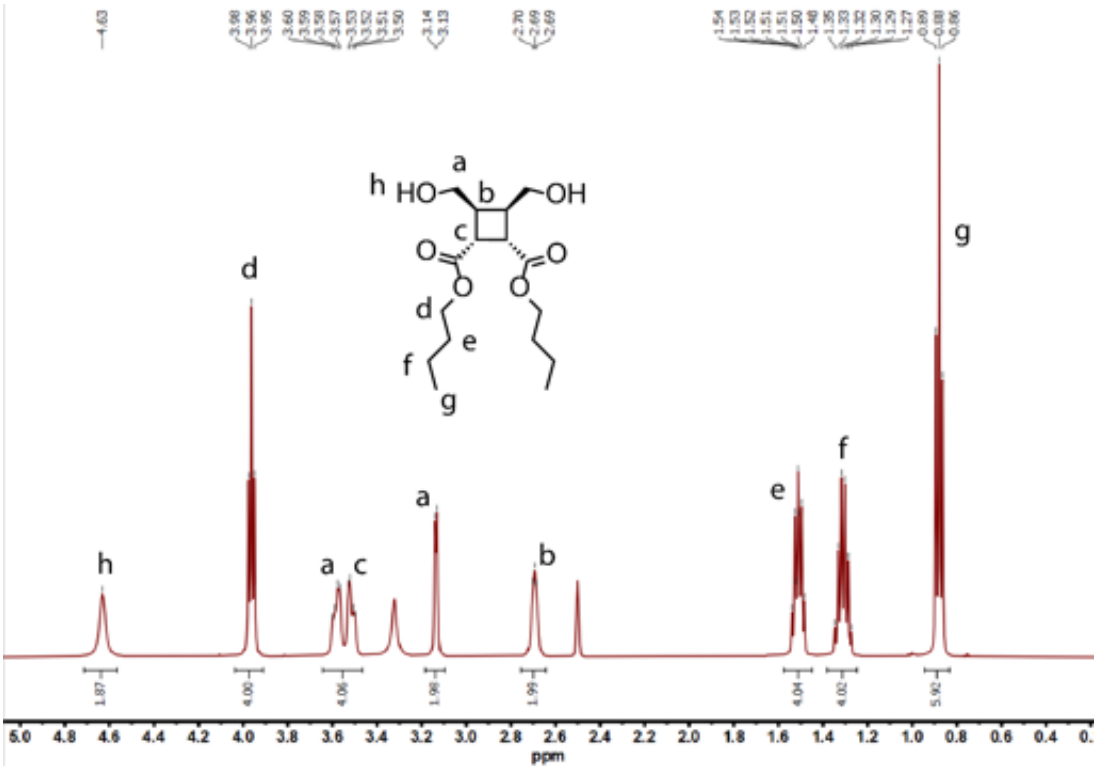

^{1}H NMR (500 MHz, DMSO-d6) spectrum of **2c**

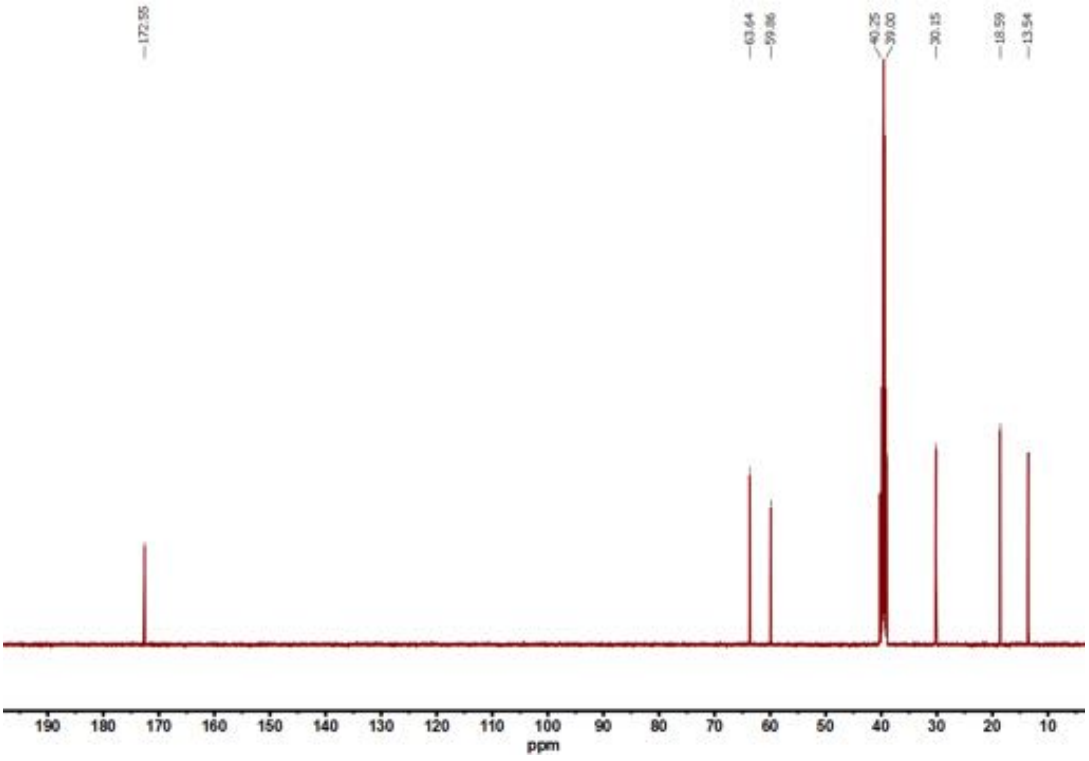

^{13}C NMR (125 MHz, DMSO-d6) spectrum of compound **2c**

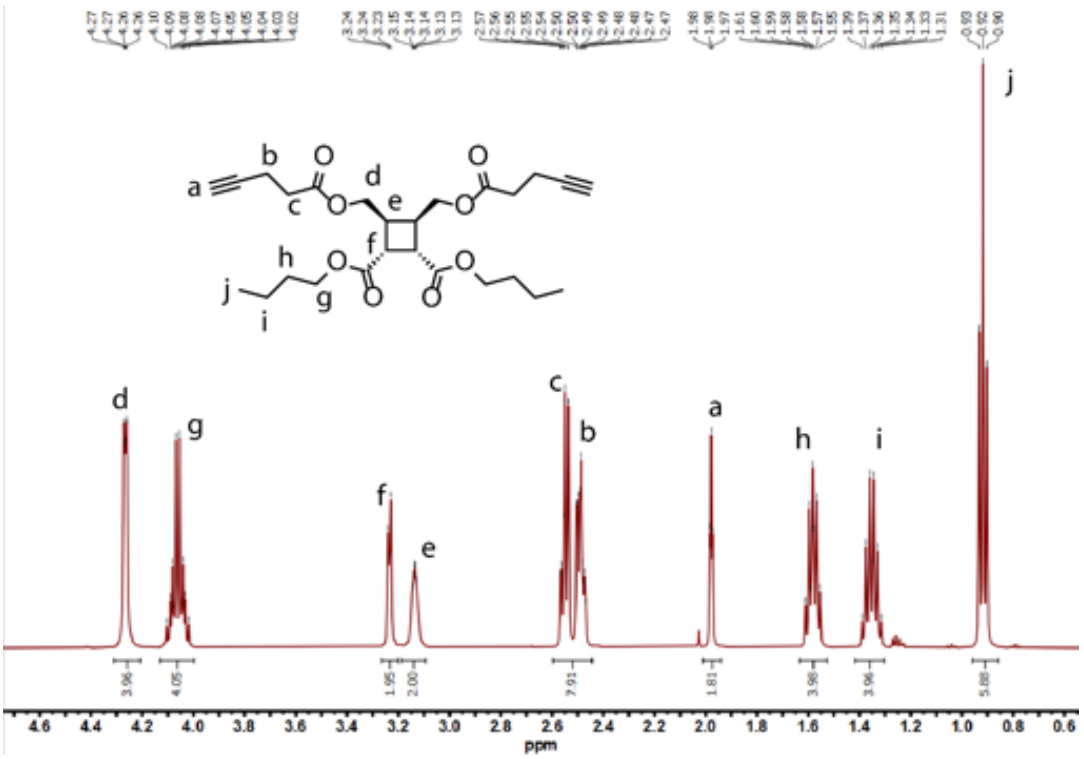

^{1}H NMR (500 MHz, $CDCl_3$) spectrum of **2**

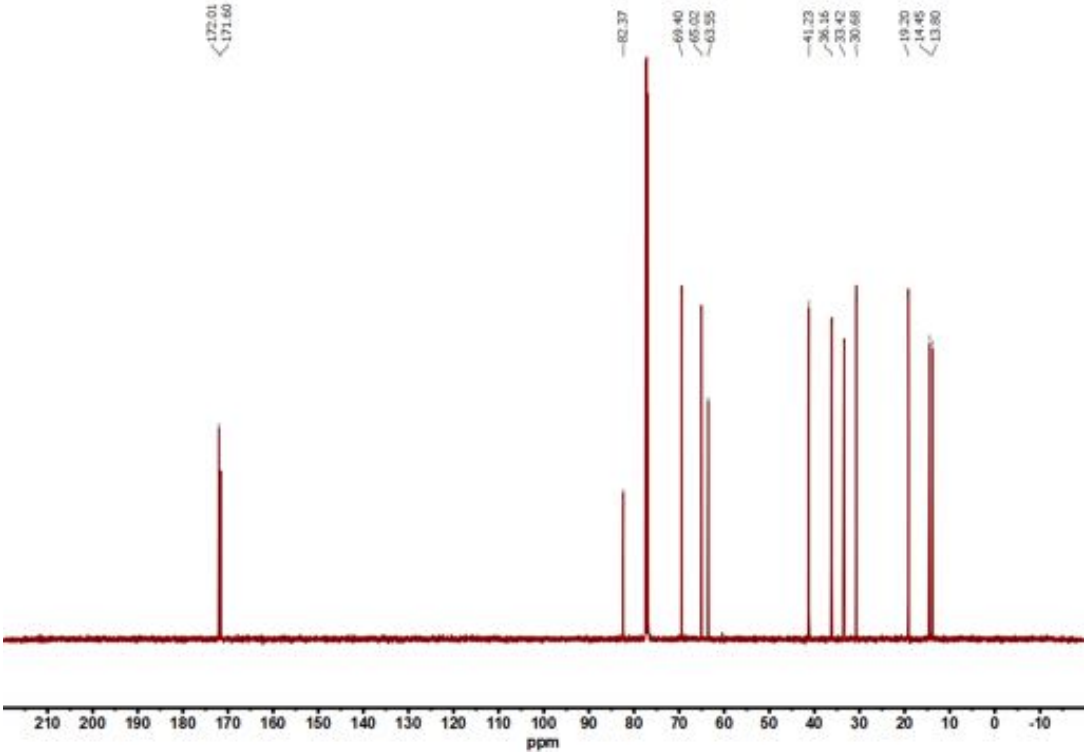

^{13}C NMR (125 MHz, $CDCl_3$) spectrum of compound **2**

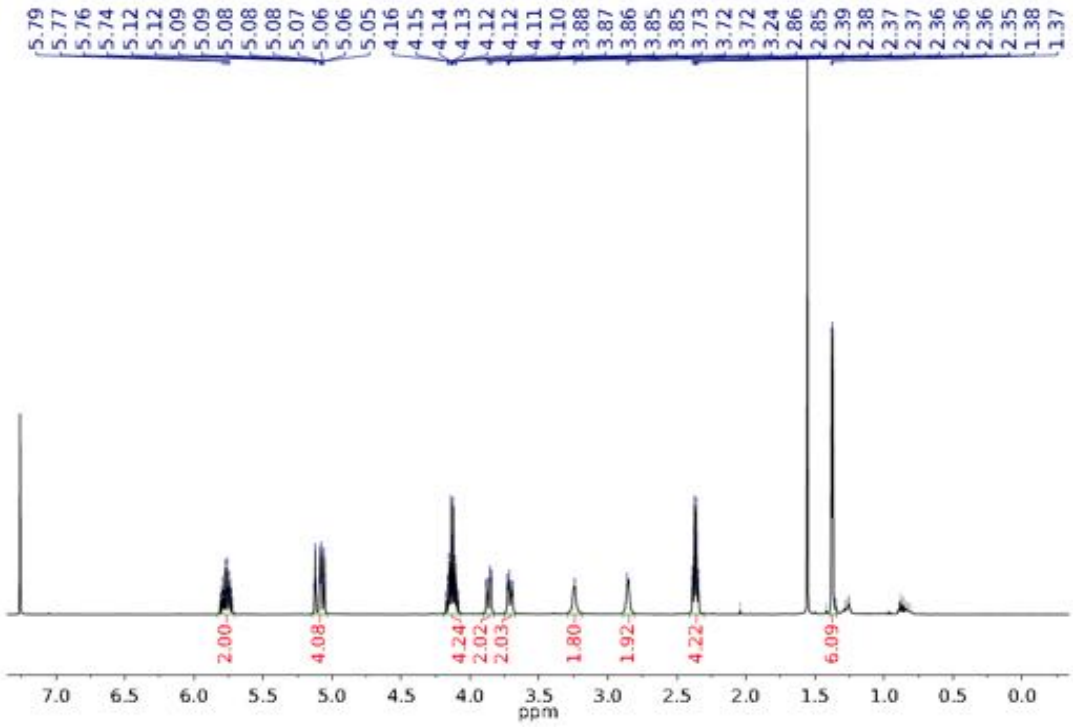

^{1}H NMR (500 MHz, $CDCl_3$) spectrum of **IIb**

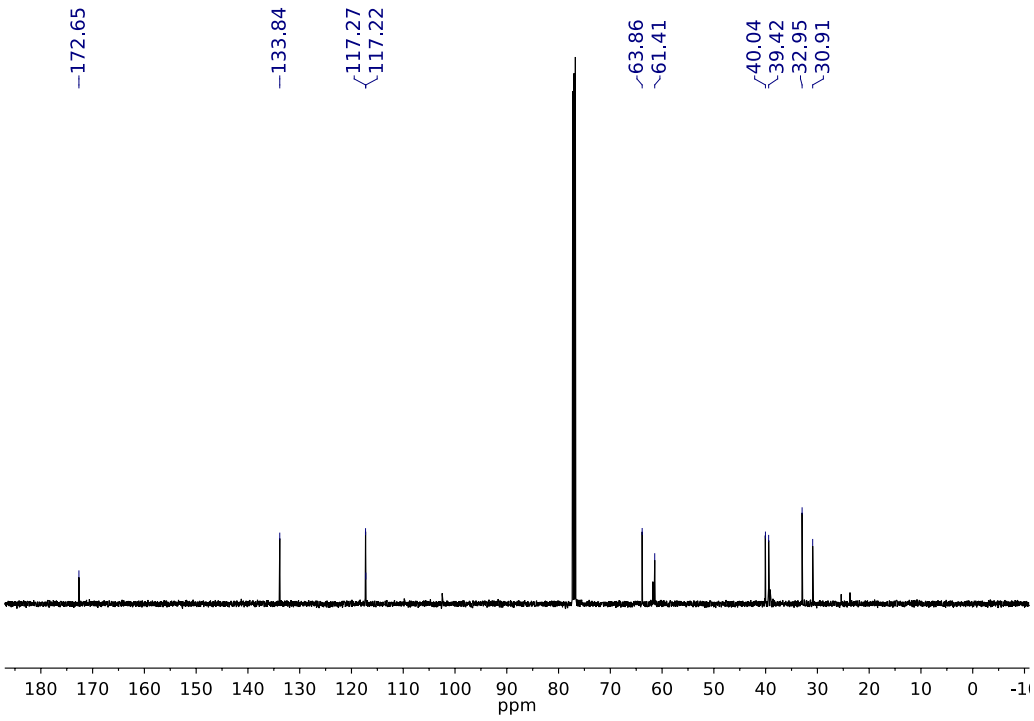

^{13}C NMR (125 MHz, $CDCl_3$) spectrum of **IIb**

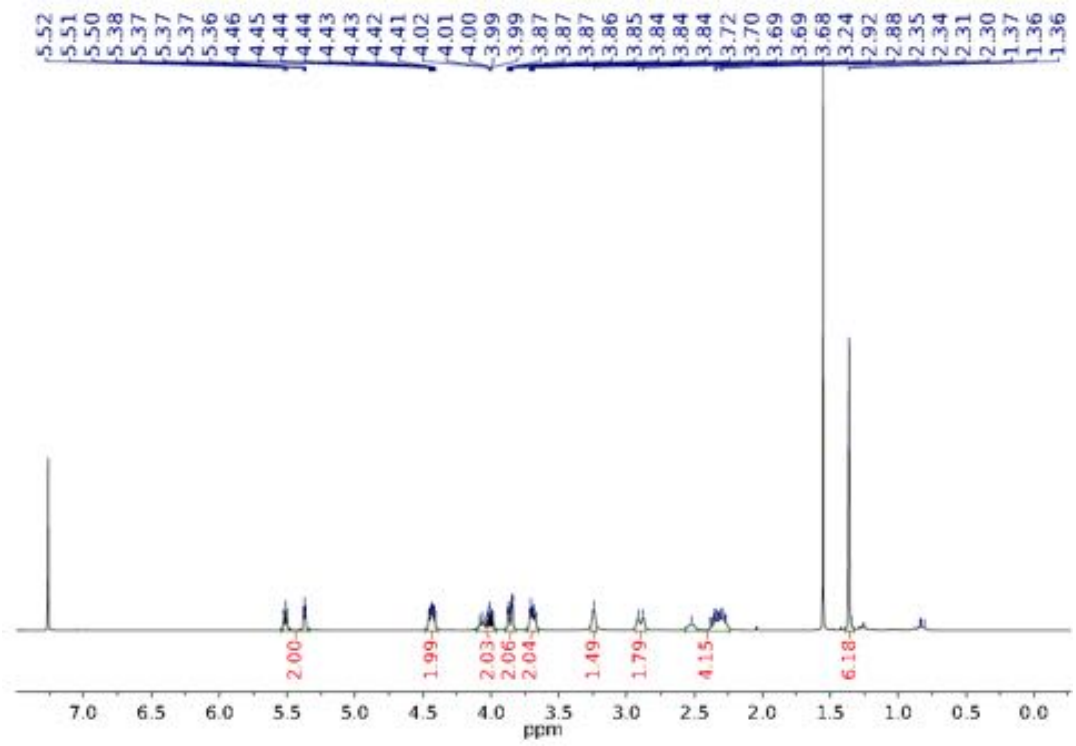

^{1}H NMR (500 MHz, $CDCl_3$) spectrum of **IIc**

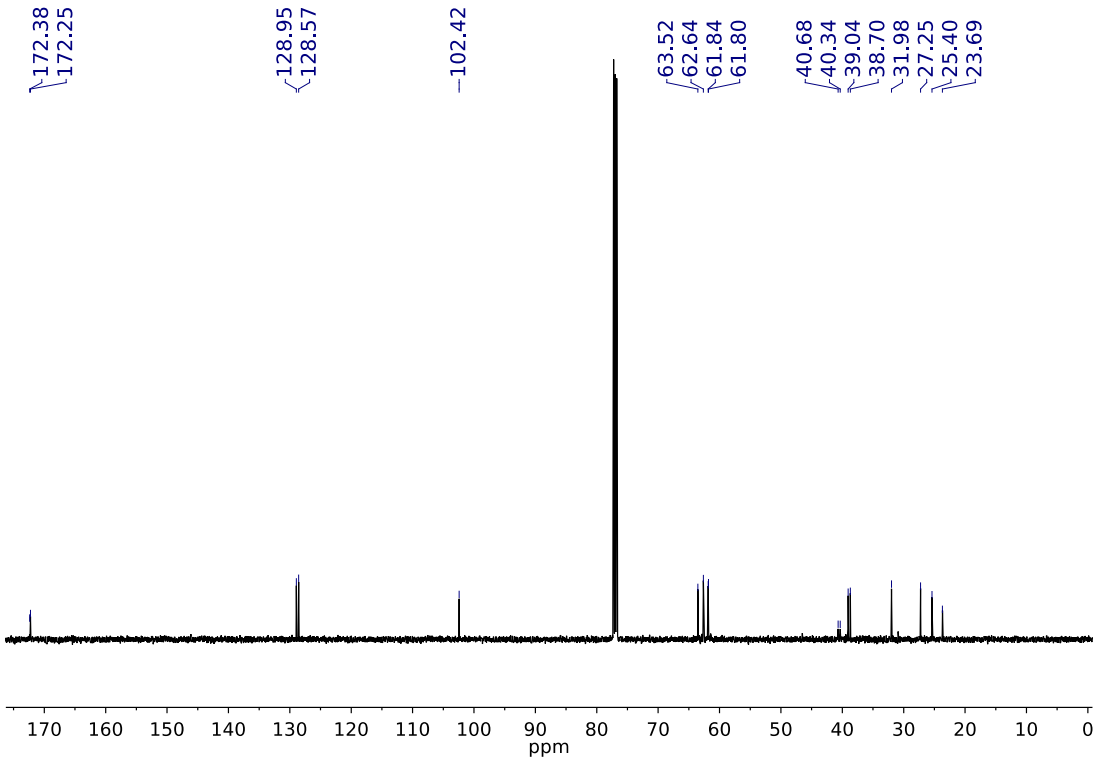

^{13}C NMR (125 MHz, $CDCl_3$) spectrum of **IIc**

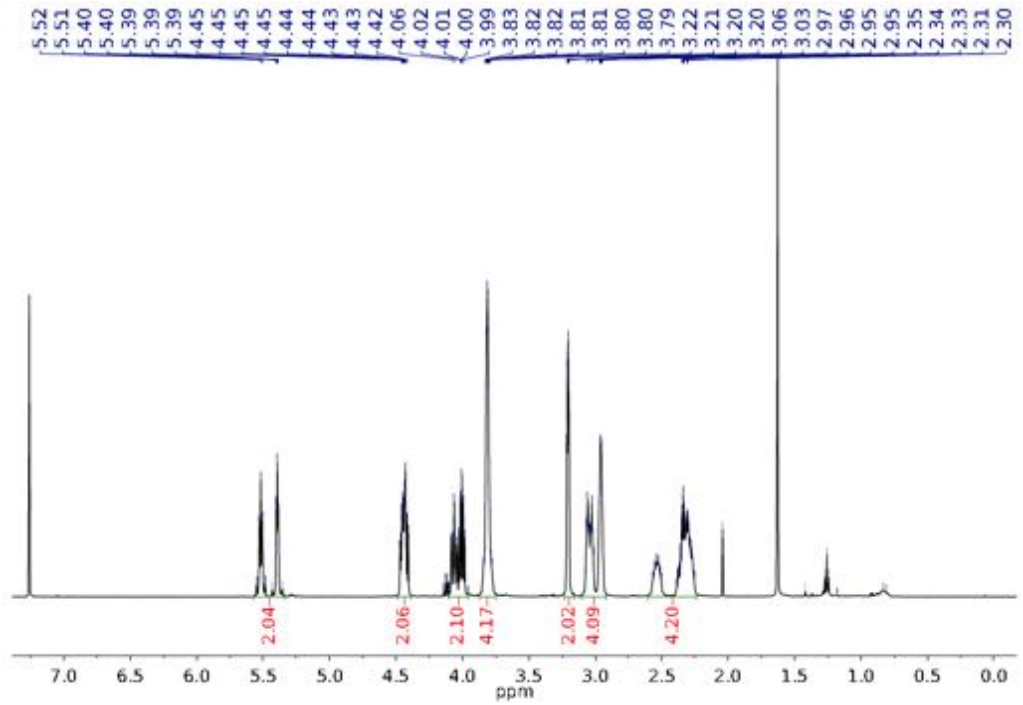

^{1}H NMR (500 MHz, $CDCl_3$) spectrum of **IId**

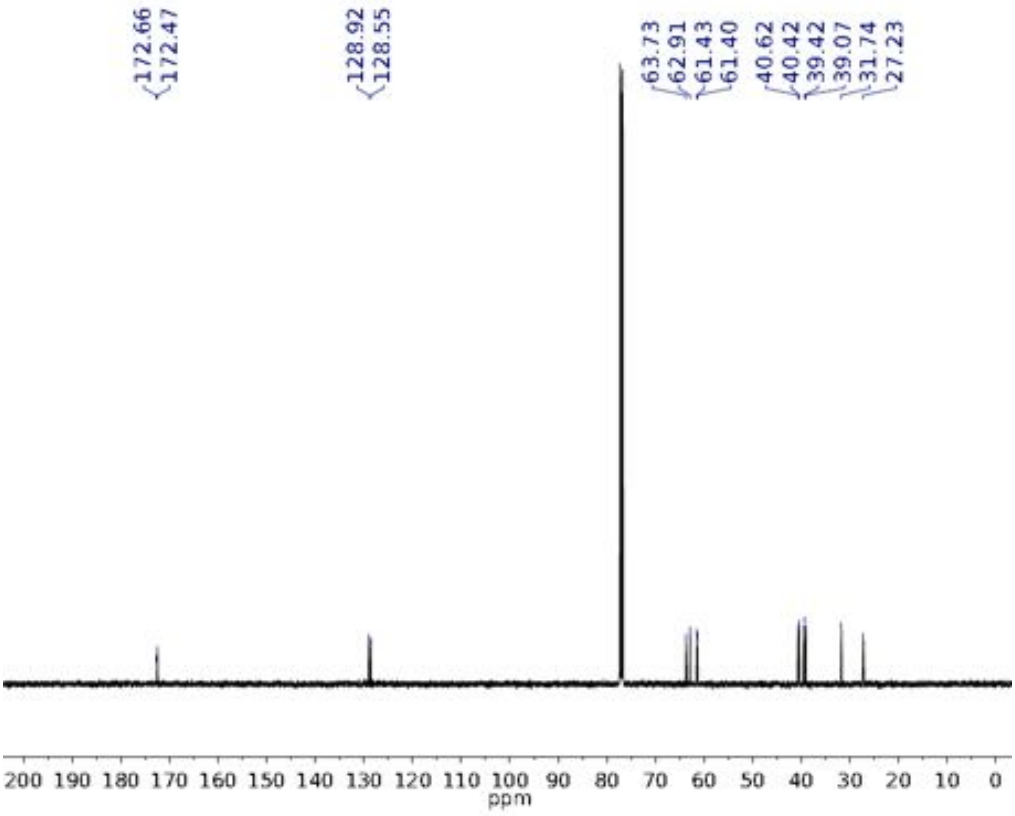

^{13}C NMR (125 MHz, $CDCl_3$) spectrum of **IId**

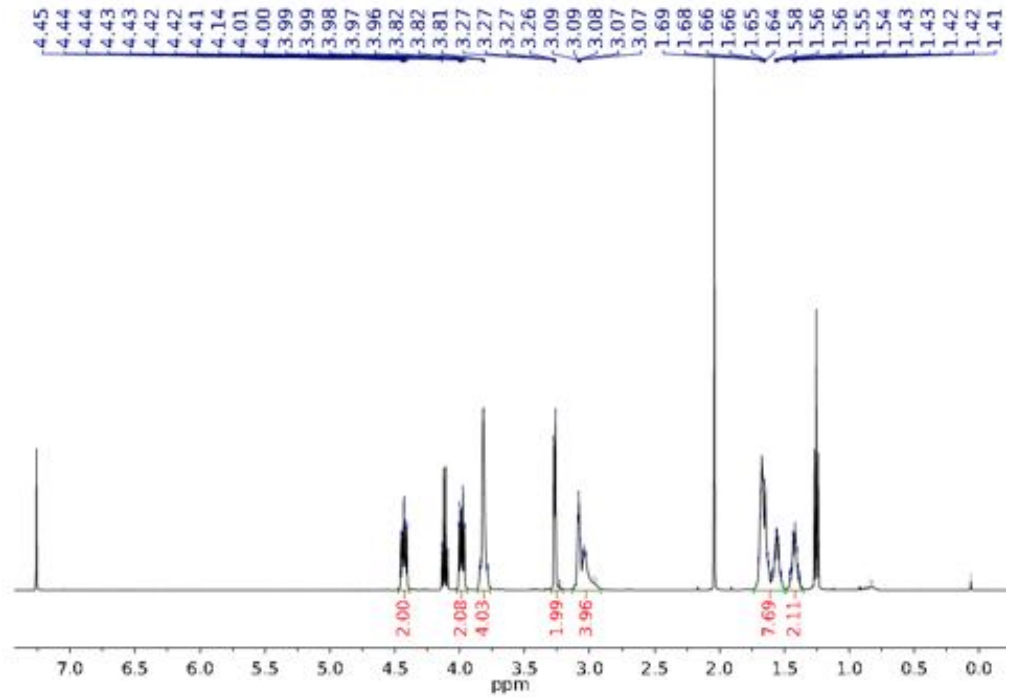

^{1}H NMR (500 MHz, $CDCl_3$) spectrum of **IIe**

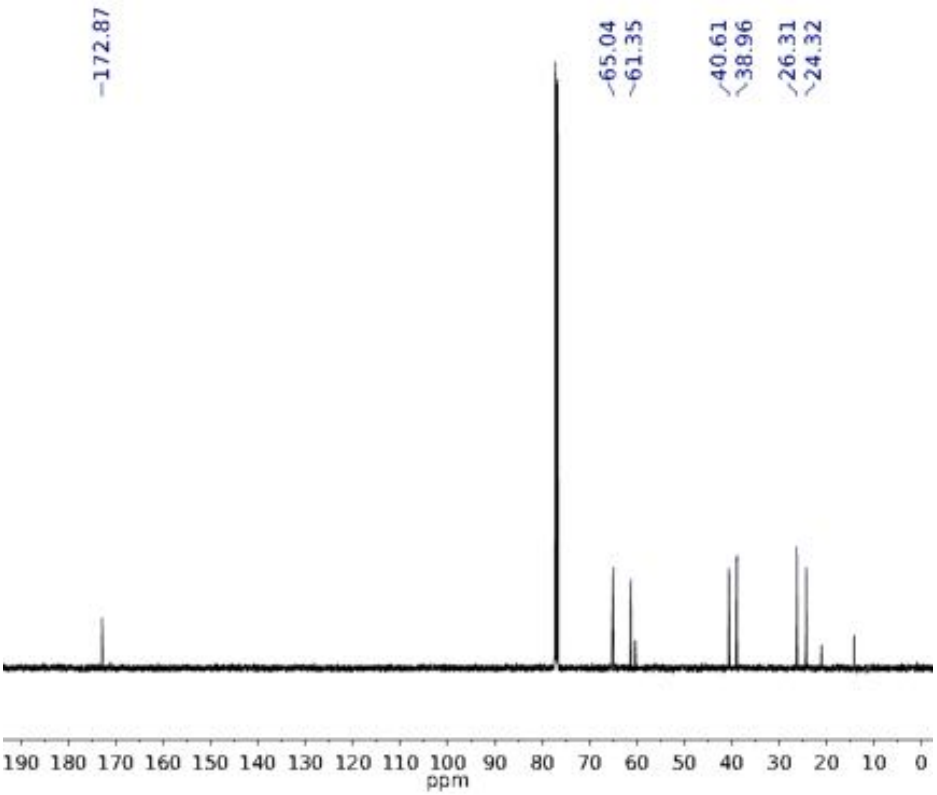

^{13}C NMR (125 MHz, $CDCl_3$) spectrum of **IIe**

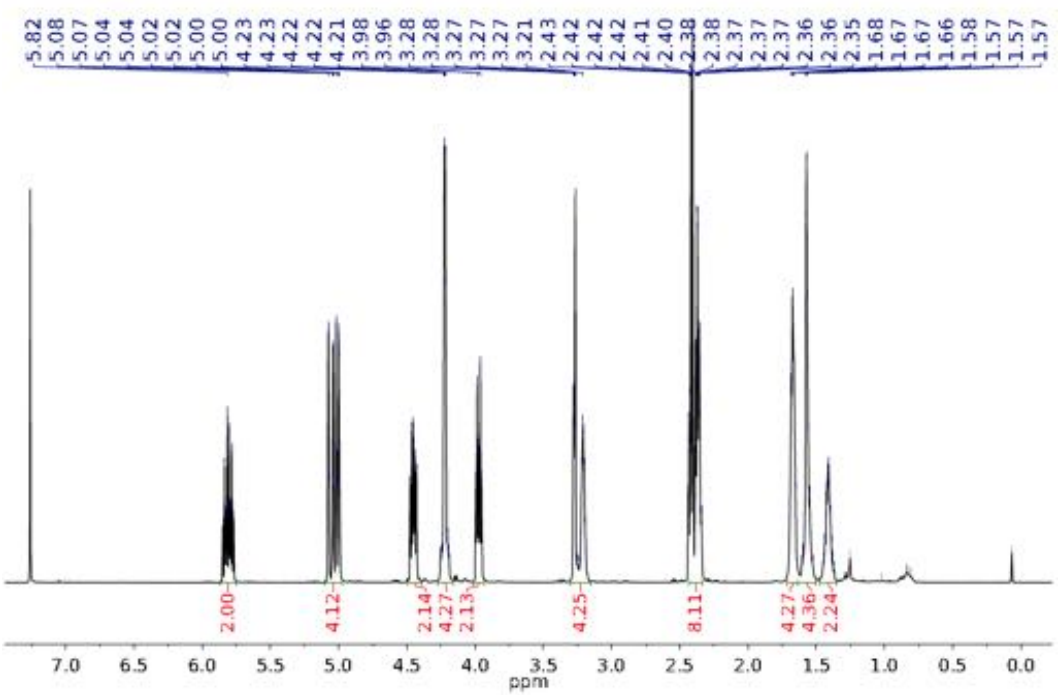

^{1}H NMR (500 MHz, $CDCl_3$) spectrum of **IIf**

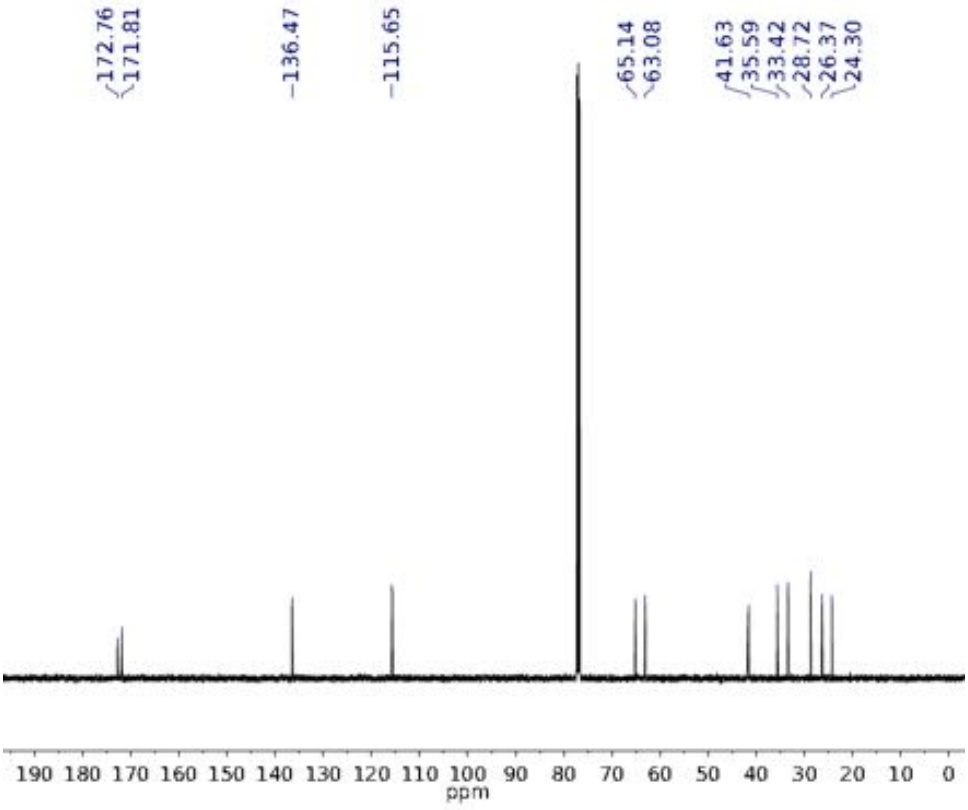

^{13}C NMR (125 MHz, $CDCl_3$) spectrum of **IIf**

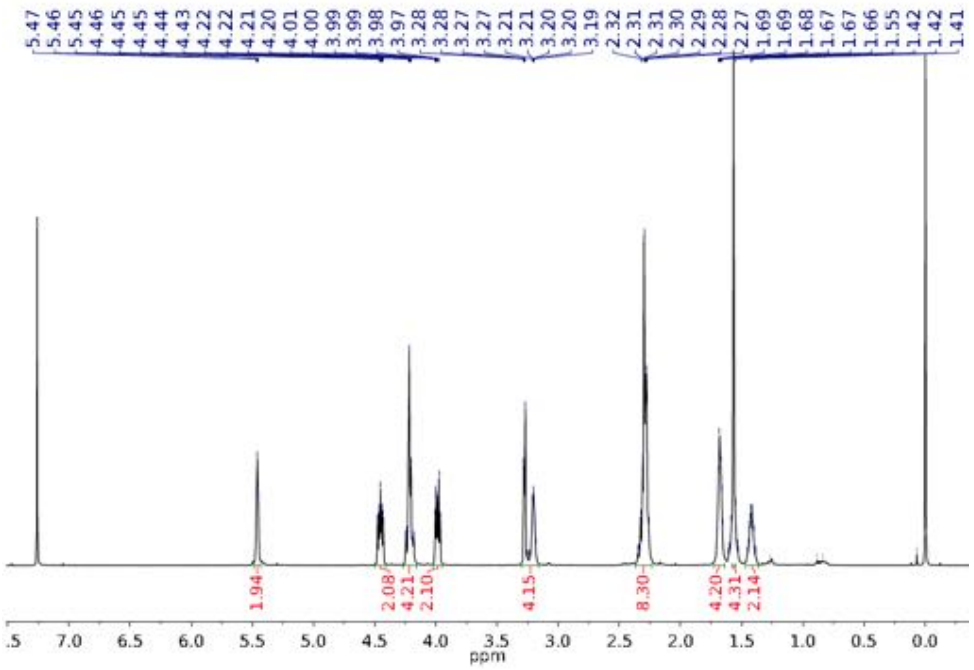

^{1}H NMR (500 MHz, $CDCl_3$) spectrum of **IIg**

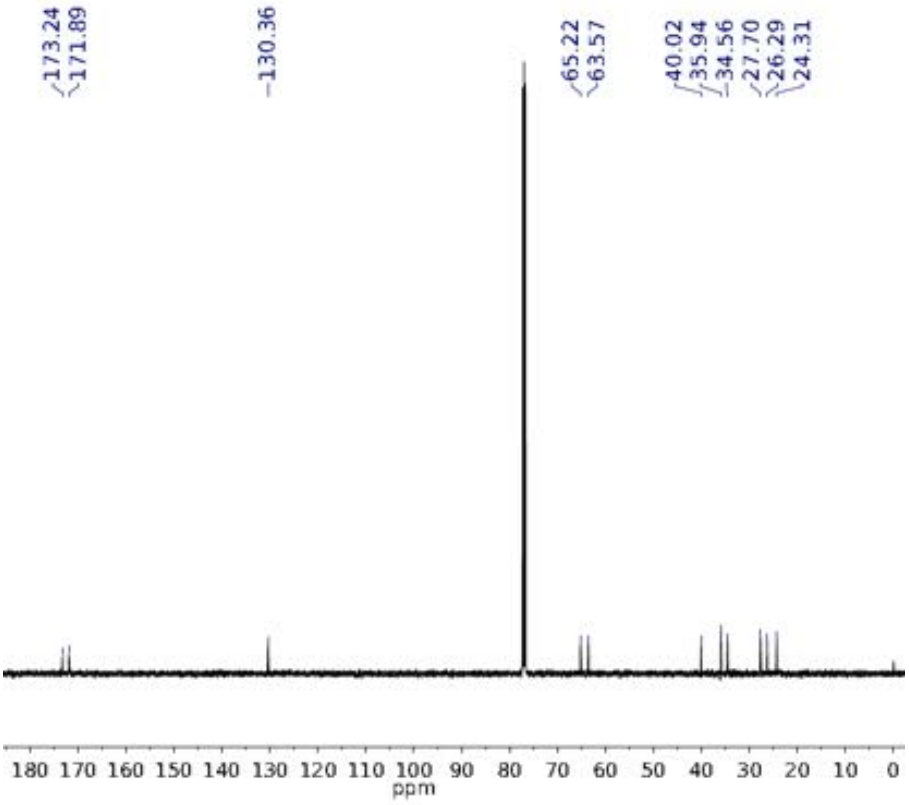

^{13}C NMR (125 MHz, $CDCl_3$) spectrum of **IIg**

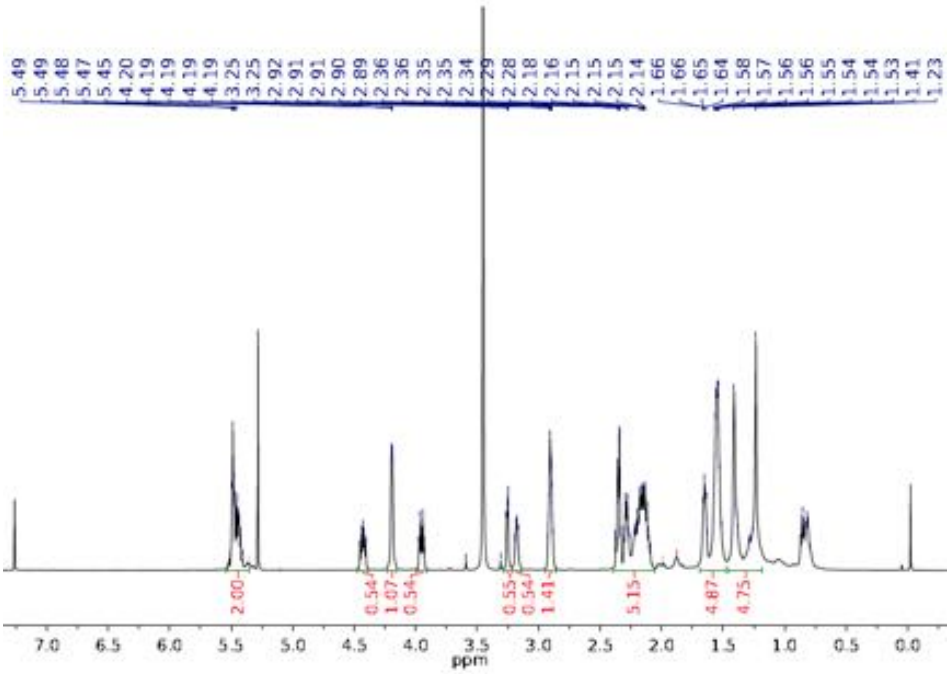

^{1}H NMR (500 MHz, $CDCl_3$) spectrum of polymer **PII**

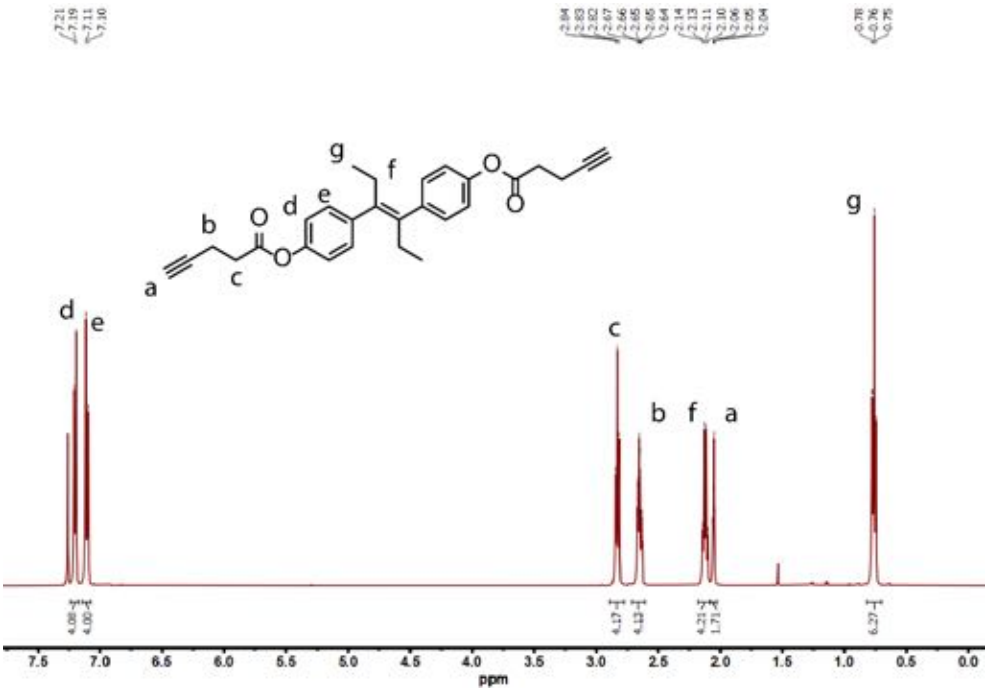

^{1}H NMR (400 MHz, $CDCl_3$) spectrum of **3**

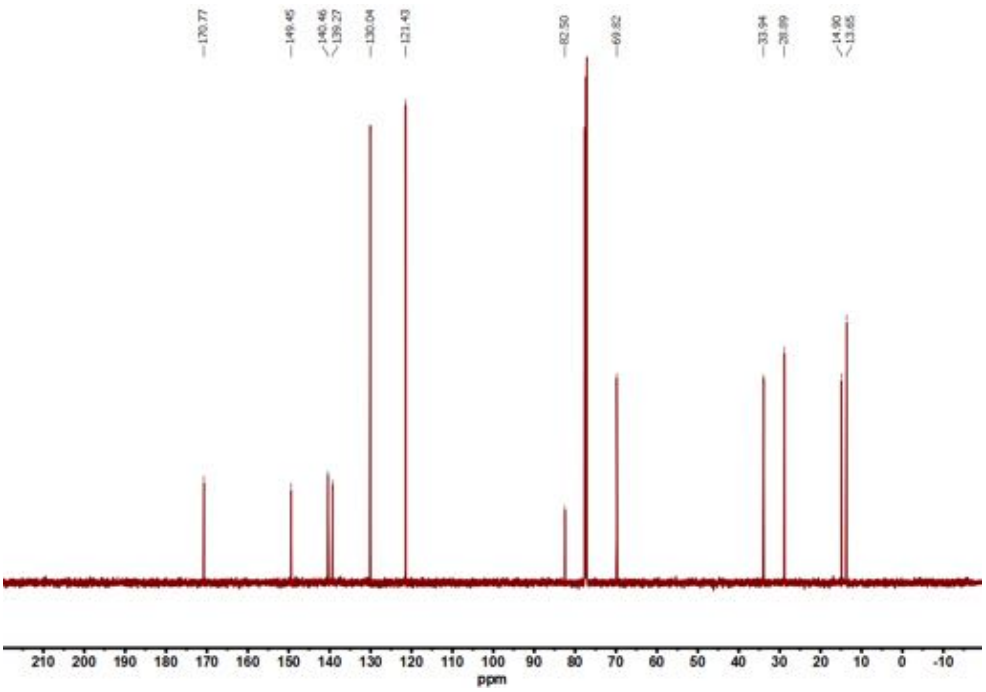

^{13}C NMR (100 MHz, $CDCl_3$) spectrum of **3**

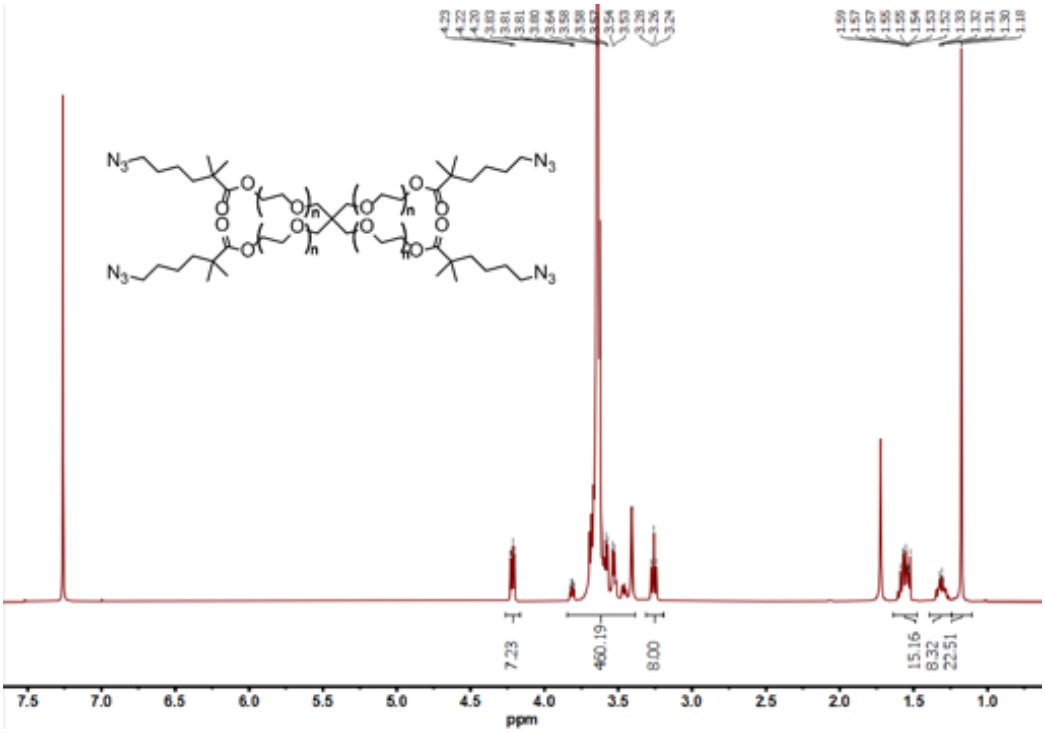

^{1}H NMR (400 MHz, $CDCl_3$) spectrum of azide-terminated 4-arm PEG

VI. References

(1) Wu, D.; Lenhardt, J. M.; Black, A. L.; Akhremitchev, B. B.; Craig, S. L. Molecular Stress Relief through a Force-Induced Irreversible Extension in Polymer Contour Length. *J. Am. Chem. Soc.* **2010**, *132*, 15936–15938.

(2) Klukovich, H. M.; Kouznetsova, T. B.; Kean, Z. S.; Lenhardt, J. M.; Craig, S. L. A Backbone Lever-Arm Effect Enhances Polymer Mechanochemistry. *Nat. Chem.* **2013**, *5* (2), 110–114.

(3) Wang, J.; Kouznetsova, T. B.; Niu, Z.; Ong, M. T.; Klukovich, H. M.; Rheingold, A. L.; Martinez, T. J.; Craig, S. L. Inducing and Quantifying Forbidden Reactivity with Single-Molecule Polymer Mechanochemistry. *Nat. Chem.* **2015**, *7* (4), 323–327.

(4) Wang, J.; Kouznetsova, T. B.; Niu, Z.; Rheingold, A. L.; Craig, S. L. Accelerating a Mechanically Driven Anti-Woodward-Hoffmann Ring Opening with a Polymer Lever Arm Effect. *J. Org. Chem.* **2015**, *80* (23), 11895–11898.

(5) Kouznetsova, T. B.; Wang, J.; Craig, S. L. Combined Constant-Force and Constant-Velocity Single-Molecule Force Spectroscopy of the Conrotatory Ring Opening Reaction of Benzocyclobutene. *Chemphyschem* **2017**, *18* (11), 1486–1489.

(6) Oberhauser, A. F.; Marszalek, P. E.; Erickson, H. P.; Fernandez, J. M. The Molecular Elasticity of the Extracellular Matrix Protein Tenascin. *Nature* **1998**, *393* (6681), 181–185.

(7) Florin, E. L.; Rief, M.; Lehmann, H.; Ludwig, M.; Dornmair, C.; Moy, V. T.; Gaub, H. E. Sensing Specific Molecular Interactions with the Atomic Force Microscope. *Biosens. Bioelectron.* **1995**, *10* (9–10), 895–901.

(8) Atkinson, S. D. M.; Almond, M. J.; Hollins, P.; Jenkins, S. L. The Photodimerisation of the α- and β-Forms of Trans-Cinnamic Acid: A Study of Single Crystals by Vibrational Microspectroscopy. *Spectrochim. Acta - Part A Mol. Biomol. Spectrosc.* **2003**, *59*, 629–635.

(9) Lin, Y.; Kouznetsova, T. B.; Craig, S. L. Mechanically Gated Degradable Polymers. *J. Am. Chem. Soc.* **2020**, *142* (5), 2105–2109.

(10) Lin, Y.; Kouznetsova, T. B.; Chang, C.-C.; Craig, S. L. Enhanced Polymer Mechanical Degradation through Mechanochemically Unveiled Lactonization. *Nat. Commun.* **2020**, *11*, 4987.

(11) Arora, A.; Lin, T.-S.; Beech, H. K.; Mochigase, H.; Wang, R.; Olsen, B. D. Fracture of Polymer Networks Containing Topological Defects. *Macromolecules* **2020**, *53*, 7346–7355.

(12) Zhong, M.; Wang, R.; Kawamoto, K.; Olsen, B. D.; Johnson, J. A. Quantifying the Impact of Molecular Defects on Polymer Network Elasticity. *Science* **2016**, *353* (6305), 1264–1268.

(13) Rivlin, R. S.; Thomas, A. G. Rupture of Rubber. I. Characteristic Energy for Tearing. *J. Polym. Sci.* **1953**, *10* (3), 291–318.